



# The XNA alphabet

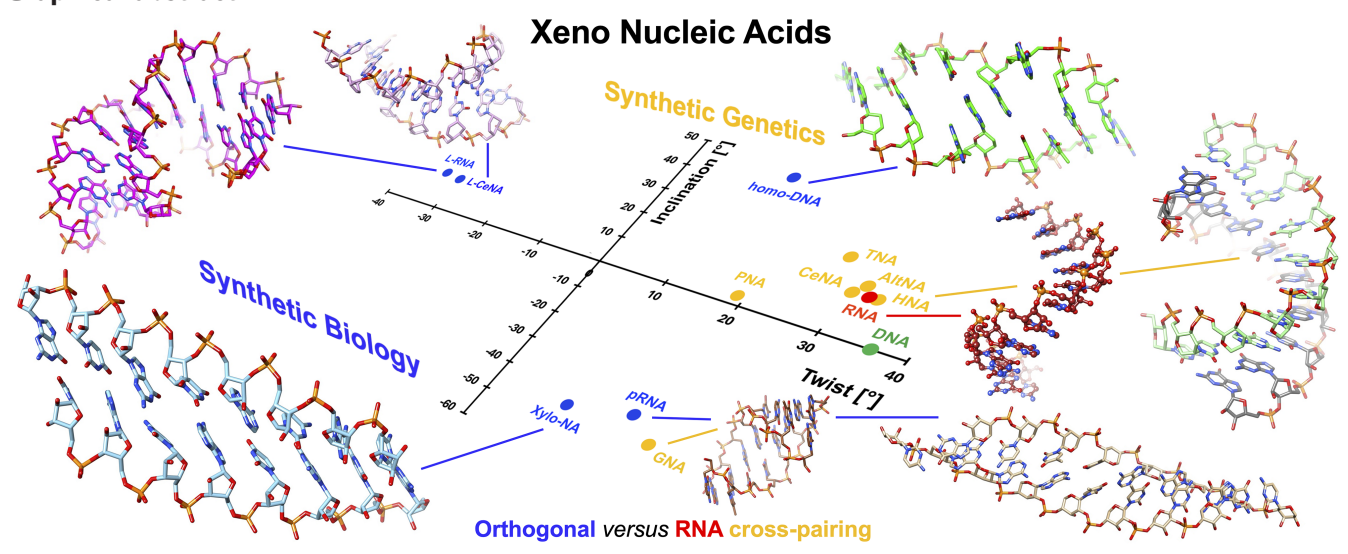
John C. Chaput <sup>1,2,3,4,\*</sup>, Martin Egli <sup>5,\*</sup>, Piet Herdewijn <sup>1,6,\*</sup>

- <sup>1</sup>Department of Pharmaceutical Sciences, University of California, Irvine, CA 92697-3958, United States
- <sup>2</sup>Department of Chemistry, University of California, Irvine, CA 92697-3958, United States
- <sup>3</sup>Department of Molecular Biology and Biochemistry, University of California, Irvine, CA 92697-3958, United States
- <sup>4</sup>Department of Chemical and Biomolecular Engineering, University of California, Irvine, CA 92697-3958, United States
- <sup>5</sup>Department of Biochemistry, School of Medicine, Vanderbilt Ingram Cancer Center, and Vanderbilt Center for Structural Biology, Vanderbilt University, Nashville, TN 37232, United States
- <sup>6</sup>Laboratory of Medicinal Chemistry, KU Leuven, Rega Institute for Medical Research, Leuven 3000, Belgium
- \*To whom correspondence should be addressed. Email: jchaput@uci.edu
- Correspondence may also be addressed to Martin Egli. Émail: martin.egli@vanderbilt.edu
- Correspondence may also be addressed to Piet Herdewijn. Email: piet.herdewijn@kuleuven.be

#### **Abstract**

Inspired by nature, chemists have spent the last 50 years systematically designing and synthesizing a vast array of sugar-modified nucleic acids, so-called xenonucleic acids (XNAs), collectively forming what we now describe as the XNA alphabet. Within the alphabet, systems can be categorized into two major groups: those capable of interacting with natural nucleic acids and those that do not cross-pair with DNA or RNA. The sugar component of XNAs plays a crucial role in defining their conformational space, which, in turn, influences their hybridization properties and potential applications across biotechnology and synthetic biology. This review provides an overview of sugar-modified XNA systems developed to date as well as the geometric parameters and physicochemical principles that have enhanced our understanding of XNA conformational behavior, particularly in relation to their orthogonality to (i.e. inability to cross-pair with) natural nucleic acids. These insights are essential for developing a more rational approach to key processes such as XNA replication and evolution, ultimately paving the way for applications in areas including synthetic genetics, nucleic acid therapeutics, diagnostics, and nanotechnology.

### **Graphical abstract**



### Introduction

Natural nucleic acids, 2'-deoxyribonucleic acid (DNA) and ribonucleic acid (RNA), have sugar-phosphate backbones that define their duplex geometry as being helical [1] (Fig. 1). Each helical turn of DNA or RNA consists of 10–12 nucleotide (nt) units, with bases oriented either perpendicular (B- and Z-form DNA) or with a positive inclination (A-form DNA)

and RNA) relative to the helical axis [2, 3]. Thus, in standard B-DNA, base plane and backbone adopt a normal orientation but in A-RNA, the backbone is negatively inclined relative to the base plane [4] (Fig. 2). Compared to other natural polymers, like proteins and carbohydrates, nucleic acids serve as informational macromolecules, storing and transmitting genetic information through well-established Watson-Crick

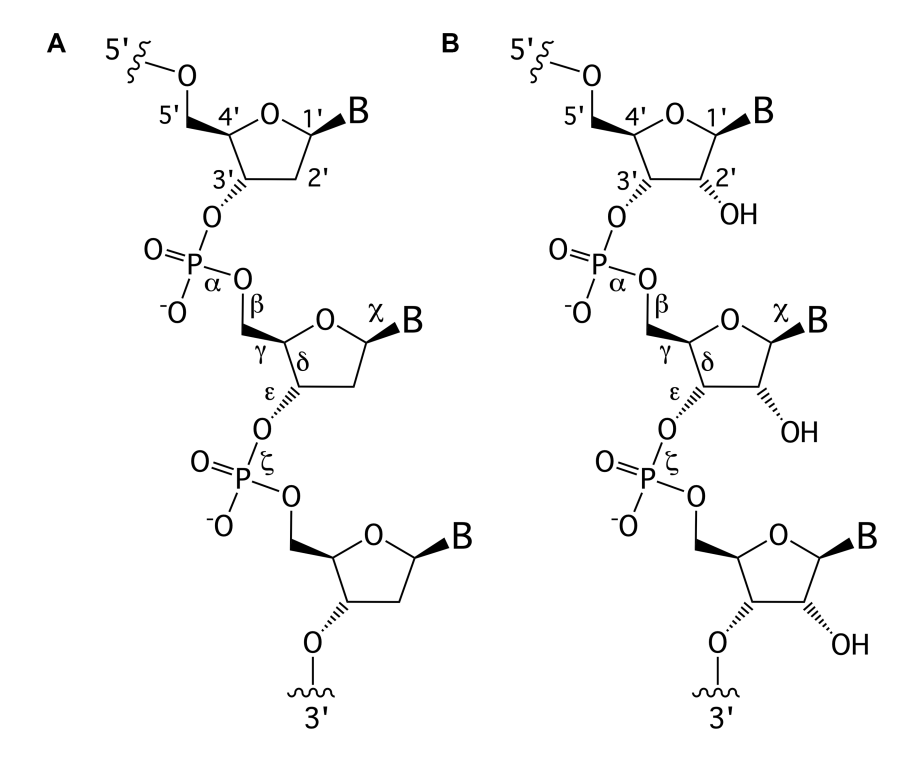


Figure 1. Structures of (A) DNA and (B) RNA. Backbone and glycosidic torsion angles are labeled..

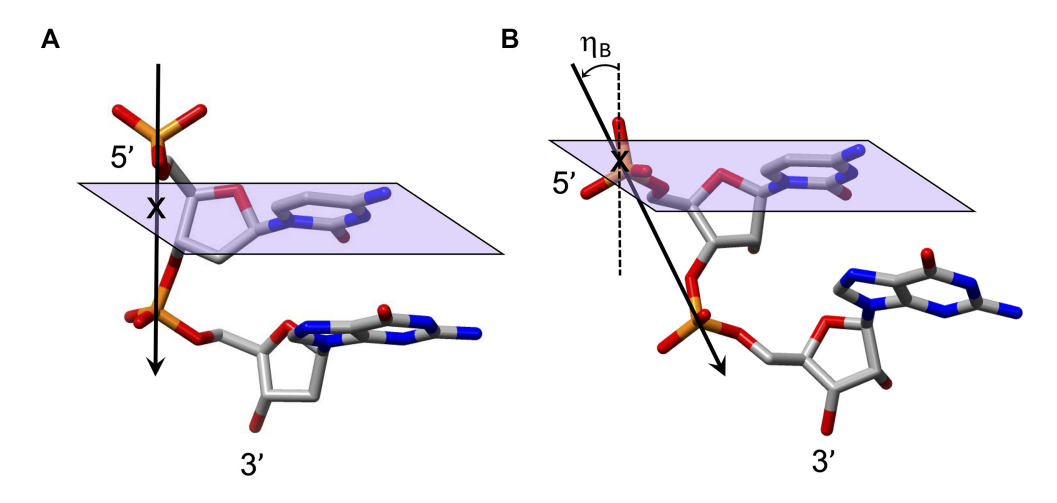


Figure 2. Illustration of the distinct degrees of backbone-base inclination in (A) B-form DNA ( $\eta_B \approx 0^{\circ}$ ) and (B) A-form RNA ( $\eta_B \cong -30^{\circ}$ ). Vectors connect adjacent phosphorus atoms, a cross marks the point where the P→P vector pierces through the plane defined by cytidine nucleobase atoms, and a dashed line indicates the normal to the plane (panel B).

base pairing rules [5, 6], which are recognized by specialized enzymes.

These fundamental principles of duplex geometry and genetic information storage also apply to artificial genetic systems known as xenonucleic acids (XNAs) [7]. Unlike natural nucleic acids, XNAs feature chemically modified backbones in which the deoxyribose or ribose sugar found in DNA and RNA, respectively, is replaced with an alternative sugar moiety [8, 9]. The rationale for such modifications is to develop synthetic genetic polymers with unique physicochemical properties that can be studied in basic and applied areas of science. In fields such as synthetic biology, materials science, and drug discovery, XNAs are valued for their potential advantages (Fig. 3), including increased hybridization stability, enhanced chemical resistance, and elevated resistance against biological nucleases [10-12]. Fundamental areas, including studies into the origins of life, examine XNAs as progenitor candidates of RNA [13].

Studies into the origin of nucleic acid structure have shown that some XNAs exhibit base-pairing stability comparable to or even superior to natural DNA and RNA [14]. For instance, the melting temperature (T<sub>m</sub>) of a β-D-2′,3′dideoxyglucopyranosyl nucleic acid (homo-DNA) dodecamer duplex was over 30°C higher than that of its DNA counterpart [15]. This suggests that maximum pairing strength alone was unlikely to be the primary factor in nature's selection of RNA as the foundation of life's genetic system [16]. Instead, accuracy and uniformity of base pairing in a biologically relevant environment were likely more critical factors.

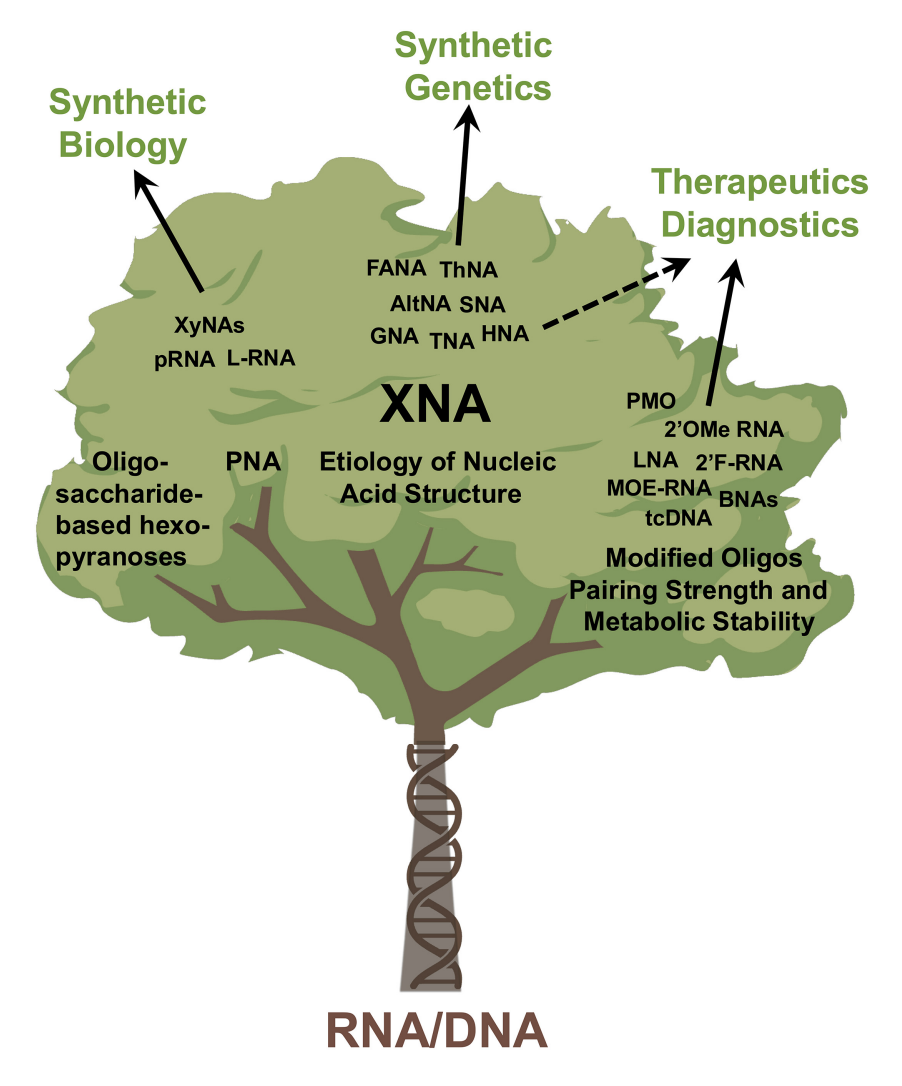


Figure 3. Emerging branches and applications of XNA beyond DNA and RNA. Only selected examples are shown on individual branches and the list is by no means exhaustive.

Most XNA applications developed to date require the faithful recognition of XNA by natural DNA and RNA [17–19]. For XNAs to functionally interact with DNA and RNA, they must be capable of forming helical structures resembling natural antiparallel Watson-Crick duplexes [8]. Researchers have explored four main strategies for engineering XNAs that can hybridize with natural nucleic acids:

- Chemical modification of natural nucleic acids to enhance hybridization strength and enzymatic stability [8], leading to the discovery of locked nucleic acid (LNA) [20], 2'-O-(2-methoxyethyl)-RNA (MOE-RNA) [21, 22], and 2'-deoxy-2'-fluoroarabino nucleic acid (FANA) [23, 24].
- 2. Biomimetic approaches using oligopeptides as structural models, inspired by the helical properties of  $\alpha$ -helices in proteins. Although  $\alpha$ -helices differ geometrically from nucleic acid helices, modifications have enabled the development of peptide nucleic acids (PNAs), which can form stable duplexes with DNA and RNA [25]. A particular characteristic of PNA is that it is charge neutral, which allows it to invade double-stranded (ds) DNA [26].

- 3. Carbohydrate-based designs using oligosaccharides as structural templates. While natural polysaccharides like amylose adopt helical conformations, their geometries typically do not align with DNA/RNA [27]. However, systematic studies of carbohydrate modified nucleic acids led to the discovery of hexitol nucleic acid (HNA), which maintains a helical structure and basepairing compatibility with DNA and RNA [28].
- 4. Prebiotic chemistry-inspired designs, exploring alternative nucleic acid backbones that could have arisen in a pre-RNA world. This approach led to the discovery of threose nucleic acid (TNA), which can form stable antiparallel duplexes with DNA and RNA despite its backbone being one atom shorter per repeating unit [29].

This review focuses on sugar-modified XNAs and provides a tabulated summary of most of the XNAs synthesized to date and investigated to various degrees with regards to pairing preference and stability. A majority of such XNAs retains hybridization compatibility with natural nucleic acids—highlighting their potential in genetic applications. In this context, synthetic genetics refers to engineered nucleic acids capable of interacting with DNA and RNA to modulate their functions. In contrast, synthetic biology, particu-

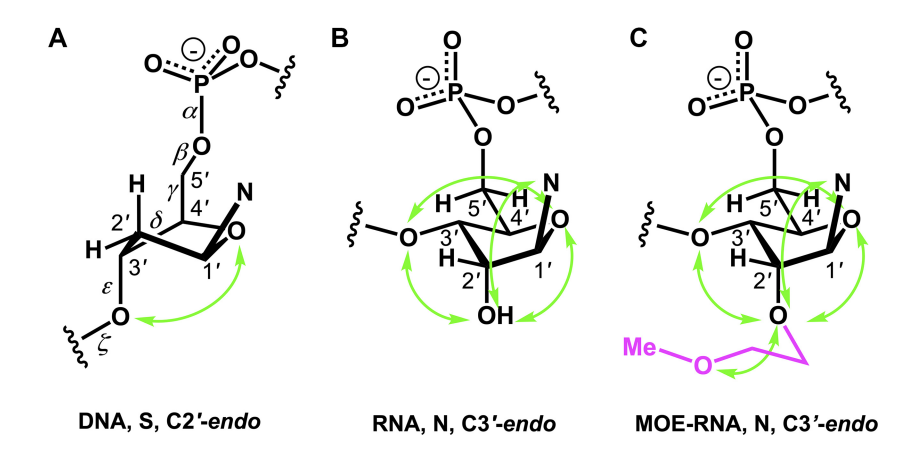


Figure 4. Gauche effects indicated by green arrows in the sugar rings of (A) 2'-deoxyribonucleotides (one), (B) ribonucleotides (four), and (C) 2'-O-(2-methoxyethyl)-RNA (MOE-RNA) (five).

larly from a chemical perspective, aims to develop orthogonal genetic systems that operate independently of natural nucleic acids. To this end, researchers have also designed sugarmodified, non-cross-pairing XNAs such as pyranosyl-RNA (pRNA) [30], xylonucleic acid (XyNA) [31], and L-RNA [32]. These systems serve diverse purposes, from exploring the origins of life (e.g. pRNA) to designing nucleic acids with enhanced enzymatic stability for aptamer applications (e.g. L-RNA) and materials science. In the context of synthetic biology and L-RNA/-DNA, some researchers have warned of potentially overlooked risks related to the creation of mirror life. They have called for a broader discussion of the potential creation of lifeforms completely based on mirror-image biological molecules such as DNA and RNA composed of "left-handed nucleotides" and proteins composed of "righthanded" amino acids [33].

In this Critical Perspective and Review, we discuss the geometric parameters including sugar conformation, helicity, helical rise and twist, backbone-base inclination and biophysical features that form the basis for an XNA's ability to cross-pair with the natural nucleic acids or, alternatively, form a stable orthogonal pairing system of potential interest in the pursuit of synthetic biology. Examples of particular XNAs either of the RNA/DNA cross-pairing type or constituting an orthogonal system, are examined in the contexts of pairing stability and 3D structure. Further, the review discusses the state-of-the-art of XNA polymerase development and selected applications of XNAs in the discovery and development of oligonucleotide therapeutics.

#### DNA—the most famous XNA

The primary difference between DNA and RNA is the absence of a hydroxyl group at the 2'-position of the sugar, a fundamental distinction in molecular design (Fig. 1). RNA is considered the first nucleic acid polymer to support life due to its ability to both catalyze chemical reactions (phenotype) and store genetic information (genotype). However, its chemical instability limits RNA genomes in extant life to RNA viruses. Removing the 2'-hydroxyl group results in a more chemically stable polymer that is better suited for storing and transferring genetic information. This transition is supported by considerations of life's origin and present-day cellular biochemistry. Notably, prebiotic synthesis of ribose is more feasible

than that of deoxyribose, and modern cells synthesize DNA building blocks from RNA precursors [34].

Thus, DNA can be regarded as the first XNA, designed by nature specifically for stable information storage with reduced catalytic activity. Nature further refined DNA by replacing RNA's uracil with thymine. (i) The removal of the 2'hydroxyl group enhances chemical stability under basic conditions but reduces stability in acidic environments, as well as the polymer's conformational diversity and catalytic potential. This occurs due to the loss of gauche effects (Fig. 4), the electron-withdrawing influence of the hydroxyl group, and the absence of anchimeric assistance in reactions like hydrolysis [35]. (ii) The substitution of thymine with uracil also decreases the acidity of the base moiety (pKa of thymine in thymidine  $\sim$ 9.8 versus uracil in uridine  $\sim$ 9.2), suggesting that uracil in RNA may more readily facilitate catalytic activity through deprotonation [36]l. (iii) Cytosine deamination in DNA results in uracil which, if not repaired before replication, leads to a G:C to A:T transition mutation. Repair of U in DNA proceeds via a base-excision pathway initiated by uracil DNA glycosylase [37]. (iv) Due to its function to store genetic information, DNA has a longer lifespan than RNA in a cell. Therefore it is important that DNA be more resistant to photochemical mutations than RNA, which further explains the use of thymine in DNA instead of uracil [38]. (v) Additionally, thymine reduces mismatch formation, improving DNA's ability to faithfully replicate its genetic information, which was essential at life's origin. (vi) The methyl group in thymine also stabilizes the DNA duplex through base stacking, though its evolutionary significance remains unclear. (vii) The 5-methyl group, always present in in DNA but occurring in RNA only as a modification (m5U), may also have been introduced as a factor to contribute to hydrophobic interactions with protein side chains, and influence groove widths and flexibility of dsDNA for similar reasons (i.e. groove recognition by DNA metabolic enzymes) [39].

### RNA—functional role in biology

RNA holds a unique position among biopolymers due to its distinct physicochemical properties, which are largely attributed to the presence of a ribofuranose sugar in its repeating nucleotide unit. In RNA, the sugar moiety consists of four oxygen atoms, one anomeric nitrogen atom, and five carbon

atoms. These atoms are arranged such that each heteroatom is part of at least one X-C-C-Y system, where conformational preferences are governed by the gauche effect.

In ribose (ribonucleotides), four types of gauche effects occur within the five-membered ring, whereas in 2'-deoxyribose (2'-deoxyribonucleotides), only one gauche effect contributes to the pseudorotational equilibrium of the sugar ring (Fig. 4A and B). A simplification is made here regarding the fifth gauche effect (O5'-C5'-C4'-O4'), which has minimal influence on sugar conformation.

The gauche effect is stronger than the anomeric effect, and in 2'-deoxyribonucleotides (DNA), these effects counteract each other, leading the DNA sugar to adopt a South (S-type) conformation [40]. In contrast, in TNA (Table 1), two gauche effects (O2'-C2'-C1'-O4' and O3'-C3'-C4'-O4') and one anomeric effect (O2'-C2'-C1'-N) act in the same direction, stabilizing the sugar in an N-type C4'-exo conformation [41–43]. The role of the gauche effect in nucleic acid preorganization is further illustrated by 2'-O-(2-methoxyethyl)-RNA (MOE-RNA) [21, 22, 44, 45], where the 2'-O-(2-methoxyethyl) moiety undergoes preorganization thanks to an additional gauche effect in the substituent (Fig. 4C), thereby enhancing duplex stability together with a water molecule bound between O2', O3', and the outer oxygen of the MOE substituent.

 $N3' \rightarrow P5'$  phosphoramidate DNA, where O3' is replaced by an amino group, bridges the properties of DNA and RNA. The presence of N3' weakens the gauche effect between O3' and O4', which is present in DNA (Fig. 4A), shifting the N-S pucker equilibrium to an RNA-like C3'-endo conformation [46]. The crystal structure of a fully modified phosphoramidate DNA dodecamer duplex confirmed that all amino sugars adopt the C3'-endo pucker. This structure also reveals an extensive hydration network around the backbone, facilitated by the 3'-NH group [47]. Additionally, amino groups interact with chloride anions, distinguishing the N3' hydrogen from its lone pair, which is positioned for maximum overlap with the antibonding P-O5' σ\* orbital. This highlights the significance of the anomeric effect in DNA and RNA backbones and underscores the favorable stereoelectronics underlying the g-/g- conformation of  $\alpha/\zeta$  torsion angles around the P-O5' and O3'-P bonds (Figs. 1,4). Notably, phosphoramidate DNA not only emulates RNA conformationally but also functionally. For example, N3' $\rightarrow$ P5' phosphoramidate DNA analogs of HIV-1 TAR and RRE RNA bind tightly and specifically to the RNA-binding Tat and Rev peptides, respectively [48].

Ribonucleotides exhibit significant flexibility, in part, based on the sugar pucker C3'-endo ↔ C2'-endo equilibrium. Beyond steric effects, their sugar conformation is influenced by a complex interplay of stereoelectronic effects, including the aforementioned four gauche effects, one anomeric effect, and the electron-withdrawing impact of the 2'-OH and 3'-OH groups [40]. The strength of the anomeric effect and the N-C1'-C2'-O2' gauche effect is also base dependent. This flexibility allows RNA sugar conformation to be influenced by internal physicochemical interactions and external factors, which may contribute to the catalytic power of RNA. Such interactions include 2'-OH lone pair interactions with vicinal phosphates [40], base stacking, H-bonding, hydration, electrostatic interactions, and steric effects [49]. Additionally, modifications in the electronic properties of nucleobases affect the strength of stereoelectronic effects, which, in turn, impact sugar and phosphate conformations [50, 51]. RNA can thus be envisioned as a molecular wire, transmitting stereo-electronic effects through a cascade of orbital overlaps involving bonding, non-bonding, and antibonding orbitals [52].

2'-5'-linked RNA has a strong cross-pairing preference for RNA over DNA [53]. That 2'-5' RNA adjusts well to the structure of RNA extends to the functional realm. Thus, the concern that all RNA template-directed syntheses result in a complementary strand that contains a mixture of 2'-5' and 3'-5' linkages is lessened by the observation that functional RNAs tolerate a non-heritable 2'-5' and 3'-5' backbone heterogeneity [54]. The outcomes of MD simulations support a greater conformational flexibility of the furanose in 2'-5' linked RNA, whereby the C2'-endo is preferred over the C3'-endo pucker [55]. This is fully consistent with crystal structures of RNA duplexes that contain several 2'-5'-linked residues, i.e. most of the these display the C2'-endo pucker, but a few adopt the C3'-endo pucker [56]. Conversely, all standard 3'-5'-linked riboses show the C3'-endo pucker that is the rule in standard A-form RNA.

RNA's physicochemical uniqueness is reflected in its central biological role, particularly in catalysis. This is evident in its greater catalytic power compared to a six-membered XNA congener such as altritol nucleic acid (AltNA), as observed in intermolecular recombination experiments [57]. Whereas RNA demonstrates remarkable conformational flexibility, removing the 2'-hydroxyl group (as in DNA) results in a more rigid and well-ordered system. It is rare to find another sugar pair that achieves similar properties while retaining stable self-pairing and cross-pairing capabilities. Alternative sugar backbones, such as  $6' \rightarrow 4'$  glucopyranosyl nucleic acid, 2',3'-dideoxyglucopyranosyl nucleic acid (homo-DNA), or hydroxy-hexitol nucleic acid (AltNA), fail to replicate RNA-DNA pairing properties. Among possible alternatives, the XyloNA/dXyloNA pair comes closest, as XyloNA is relatively rigid while dXyloNA is more flexible (Fig. 5) [31, 58].

Vicens and Kieft's argument that RNA G:U, G:A, and G:G pairs should not be considered mere mismatches is reasonable, given RNA's ability to adopt an extensive range of folded structures [5]. These pairs not only fit into RNA's folding land-scape but actively enable its structural diversity. Furthermore, RNA rivals DNA in forming complex multistranded structures, including triplexes, quadruplexes, i-motifs, and Z-RNA [59]. The widespread presence of chemical modifications in RNA further directs its pairing modes [60], enhances stability and fidelity, and regulates the 2'-hydroxyl group's interactions with bases, base pairs, and higher-order structures.

Inside the cell, RNA exists in two major forms: messenger RNAs (mRNAs), which serve as templates for protein synthesis, and regulatory/catalytic RNAs. While mRNAs constitute only a small fraction of total RNA, ribosomal RNA (rRNA) represents the majority. Numerous noncoding RNAs have been identified, including rRNA, tRNA, miRNA, siRNA, lncRNA, circRNA, snRNA, gRNA, snoRNA, and tRFs [61]. The ligand-binding domain of riboswitches can be considered a natural RNA aptamer, and many of these RNAs are promising targets for drug discovery. Additionally, several RNA types undergo chemical modifications. For instance, 2'-O-methylation occurs in mRNA, tRNA, rRNA, and snRNA, contributing to RNA folding, structural stability, and function [62]. Such modifications, like 2'-O-methyl purine

 Table 1.
 The XNA alphabet

Abbreviation	Structure	Citation
R-ZNA	O R	[65]
S-ZNA	O D B C	[65]
4'-AlkoxNA	O P B	[66]
2'-AlkNA	O=P-O O	[67]
4'-AlkNA	O=POB B	[68]
5'-AlkNA	O P O B	[69]
AraNA	0=P-0 0=8-0 0=B-0 0-8-0 0-0 0	[70]
AltNA	NO PR	[71]
AlloNA	NO B	[14]
AltroNA	HO O P O	[14]
	R-ZNA  S-ZNA  4'-AlkoxNA  2'-AlkNA  5'-AlkNA  AraNA  AltNA  AlloNA	S-ZNA  4'-Alkoxna  4'-Alkoxna  4'-Alkna  4'-Alkna  5'-Alkna  Arana  Altna  Altna

Table 1. Continued

Name	Abbreviation	Structure	Citation
3'-Arafluoro hexitol nucleic acids	Ara-FHNA	0, B	[72]
2'-O-Alkylated nucleic acids	2'-O-AlkylNA	O B	[21]
Aminopropyl nucleic acids	R-APNA	O P R=Alkyl	[73]
	S-APNA	O NH B	[73]
2'-Amido nucleic acids	2'-AmidoNA	0 - NH NH NO O B	[74]
Apio nucleic acids	ApioNA	0=P-0 0	[75]
2'-Amino deoxynucleic acids	NH <sub>2</sub> -RNA	0=P-0 0 8 0 B 0 NH <sub>2</sub>	[76]
2'-Azido deoxynucleic acids	N <sub>3</sub> -RNA	0=P-0 0 0 B	[76]
Amido-bridged nucleic acids	AmNA	0=P-0 0 0 - NH	[77]
B BicycloDNA	BcDNA	0=P-0 0 8	[78]
		0 - 0 = 2 - 0 0 &	

Table 1. Continued

Name	Abbreviation	Structure	Citation
	Bc[3.2.1]DNA	0 B	[79]
	Bc[3.2.1]amide-DNA	O = POO E B	[80]
	Bc[4.3.0]DNA	OFF B	[81]
	2′,3′-BcNA	0 = P - 0 B	[82]
Butyl nucleic acids	BuNA	O B B	[83]
C Carbocyclic DNA	carDNA	0=P-0 0 0	[84]
Carbocyclic RNA	carRNA	O=PO OB OD-OH	[84]
Cyclohexanyl nucleic acids	CNA	0=R <sub>0</sub>	[85]
D-ribo-Cyclohexanyl nucleic acids	r-CNA	0 0 B B O O O O O O	[86]
Cyclohexenyl nucleic acids	D-CeNA	0 0 B	[87]
	L-CeNA	B	[88]

Table 1. Continued

Name	Abbreviation	Structure	Citation
Carbamate-linked nucleic acids	CarbamateNA	M H O B	[89]
D Deoxyribose nucleic acids	$\beta$ -D-DNA (Natural)	0, B	
	lpha-D-DNA	0 NB	[90]
	$\beta$ -L-DNA (mirror image DNA)	B O O M	[91]
Di-O-Methylated altropyranoside nucleic acids	DMANA		[92]
Double coding nucleic acids	DcDNA	O PO O O B	[93]
Disubstituted DNA	2',4'-DFNA	0=P0 0 B	[94]
	2'F,4'-OMe NA	0=P-0 0 RO RO B	[95]
	2′OMe,4′F NA	0 P O B O B O O O O O O O O O O O O O O O	[96]
	2′,4′-diOMe NA	O B RO B	[96]
2,4-Dihydroxycyclohexyl nucleic acids	2,4-DHCNA	O O O B	[97]
		0=6-0 0=6-0 1.8	

Table 1. Continued

Name	Abbreviation	Structure	Citation
Double-headed nucleic acids	2'-DhNA	O B OH OH OH OF POOR	[98]
Diethanol amide nucleic acids	DEANA	O N B	[99]
E Ethinyl nucleic acids	ENA	MO B	[100]
Ethylene bridged nucleic acids	EBNA	DE D	[101]
Extended nucleic acids	ExNA	O B O O O O O O O O O O O O O O O O O O	[102]
F 2'-Fluoro arabino nucleic acids	FANA	0=R <sub>0</sub>	[103]
Flexible nucleic acids	FNA	0=P-0 8	[104]
6'-Fluoro[4.3.0]bicyclo nucleic acid	6'-F-bc[4.3.0]DNA	O=POB BFODB	[105]
3'-Fluoro hexitol nucleic acids	FHNA	0 P P B	[72]
	FMHNA	0 B 0 = P O F	[106]

Table 1. Continued

Name	Abbreviation	Structure	Citation
Fluoro cyclohexenyl nucleic acids	F-h	0 B	[87]
2'-Formamido nucleic acids	2'-Formamido NA	MO B H	[107]
2'-Fluoro nucleic acids	F-RNA	0=P0	[108]
Ferrocene nucleic acids	FeNA	O=POO <sub>20</sub> Representation B Fe B	[109]
G Glycerol nucleic acids	GNA	O=R-O ,,,,O B	[110]
D-β-Gluco nucleic acids	GlucoNA	1/1. H 0 = P 0 0 0 0 0 0 0 0 0 0 0 0 0 0 0 0 0 0 0	[14]
		OSPOOH	
Glycol carbamate nucleic acids	R-GCNA	B R NH	[111]
	S-GCNA	O B NH	[111]
Glucosamino nucleic acids	3',6'-GANA	0=P00 B HO''NH2	[112]
		0 0=P-0 0 8	

Table 1. Continued

Name	Abbreviation	Structure	Citation
	4',6'-GANA	100 B	[112]
		0=P-O OH NH2	
Guanidine linked nucleic acids	GuanidineDNA	AN B	[113]
		HN R	
H Hexitol nucleic acids	α-L-HNA	1118 x	[114]
		0=P-0	
	α-D-ΗΝΑ	~ O	[115]
		0,,,_,,,,,,,,,,,,,,,,,,,,,,,,,,,,,,,,,	
	β-L-HNA	<sup>3</sup> / <sub>2</sub>	[116]
		0=P-0 0=B-0	
	β-D-HNA	mo \$	[117]
		0, , _ B 0 ≥ B − O 0 s	
Hydroxy-N-acetylprolinol nucleic acids	Hydroxy-N-AcProNA	O B	[118]
		HO	
Homo-N-deoxyribose nucleic acids	$\beta$ -D-Homo-DNA	0=P-0	[119]
		0×P-0	
	$\beta$ -L-Homo-DNA	B	[120]
		0 P=0	
	α-D-Homo-DNA	<sup>3</sup> √0 ,,B	[121]
		0=8-0	
	1'-homoDNA	wo O B	[122]
		0 - 0 - 0 - 0 -	
		Ş	

Table 1. Continued

Name	Abbreviation	Structure	Citation
5'-Hydroxyphosphonate-linked nucleic acids	5'-hpDNA	HQ O B	[123]
3'-Hydroxymethyl – aldopentopyranose nucleic acids	3'-hmAPPNA	O B B O B	[124]
I Intercalating nucleic acids	INA		[125]
Isobicyclo-DNA	IsoBcDNA	0 B	[126]
Iso-glycerol nucleic acids	IsoGNA	0 0 B 0=R-0	[127]
J, K L		r.C	
Locked nucleic acids	LNA	0 B	[20]
α-Locked NA	α-LNA	00 NB	[128]
Methylene-carbocyclo Locked NA	Methylene-cLNA	0 B	[129]
2'-O-Methoxyethyl Locked NA	cMOENA	O B CH <sub>3</sub> OCH <sub>2</sub> O B	[130]
Cyclic 2'-O-Ethyl Locked NA	cEt BNA	CH <sub>3</sub> O B	[131]

Table 1. Continued

Name	Abbreviation	Structure	Citation
Lyxo nucleic acids	2′,4′-LyxoNA	0 B	[14]
	3′,4′-LyxoNA	HO 0= P-O 0 0 0 0 0 0 0 0 0 0 0 0 0 0 0 0 0 0 0	[14]
M Morpholino nucleic acids	MorphNA (PMO)	O PO B	[132]
Mannitol nucleic acids	ManNA	0=P-N	[133]
3'-O-Methylated ANA	MANA	0=P-0 OH 0=P-0 O	[134]
2′,5′-DNA	MetaDNA	0 B	[135]
2′,5′-RNA	MetaRNA	0=P0 0 B H0 0 _	[136]
2'-O-Methoxyethyl nucleic acids	MOENA	0=P-0 0=B-0 0=P-0 0=P-0	[21]
N North Methanocarba DNA	NMDNA	H B	[137]
O Oxepane nucleic acids	OxNA	0=P-0 0	[138]

Table 1. Continued

Name	Abbreviation	Structure	Citation
P Peptide nucleic acids	PNA	HN B	[139]
Phosphoramidate nucleic acids	N3'→N5'-DNA	O B HN -	[46]
Polycarbamate nucleic acids	PCNA	O POO	[140]
Prolinol nucleic acids	ProNA	O O O O O O O O O O O O O O O O O O O	[141]
Q R Ribose nucleic acids	D-RNA (natural)	O PO O B	
	L-RNA (mirror image RNA)	0=P0 B 0 0 0 0 0 0 0 0 0 0 0 0 0 0 0 0 0 0	[142]
Ribulo nucleic acid	RibuloNA	0 P=0	[143]
S Serinol nucleic acids	SNA	HO O O	[144]
South methanocarba DNA	SMDNA	HO B	[145]
T α-L-threofuranosyl nucleic acids	TNA	HO B	[29]

Table 1. Continued

Name	Abbreviation	Structure	Citation
Threoninol nucleic acids	a-D-TNA	HN B	[146]
	a-L-TNA	THN B	[146]
Tricyclo nucleic acids	TricycloDNA	O B B	[147]
4'-Thio DeoxyNA	4'-ThioDNA	0=B-0 0 S B	[148]
4'-Thio NA	4'-ThioRNA	0=P0 S B O' OH	[149]
Triethyl amino NA	TEANA	0 = P O O O O O O O O O O O O O O O O O O	[99]
U Unlocked nucleic acids	UNA	0 B 0 OH 0 P	[150]
V Vinylpropyl nucleic acids	VPNA	0 B 0 - 0 0	[151]
W W-shape nucleic acids	WNA	0 - P-0 B	[152]

Table 1. Continued

Name	Abbreviation	Structure	Citation
X Xylo nucleic acids	XyloNA	~ O → B	[31]
Deoxyxylo nucleic acids	dXyloNA	0 - OH 0=P-O 8	[153]
Y, Z		0 _ 0=P-0 0 \$	

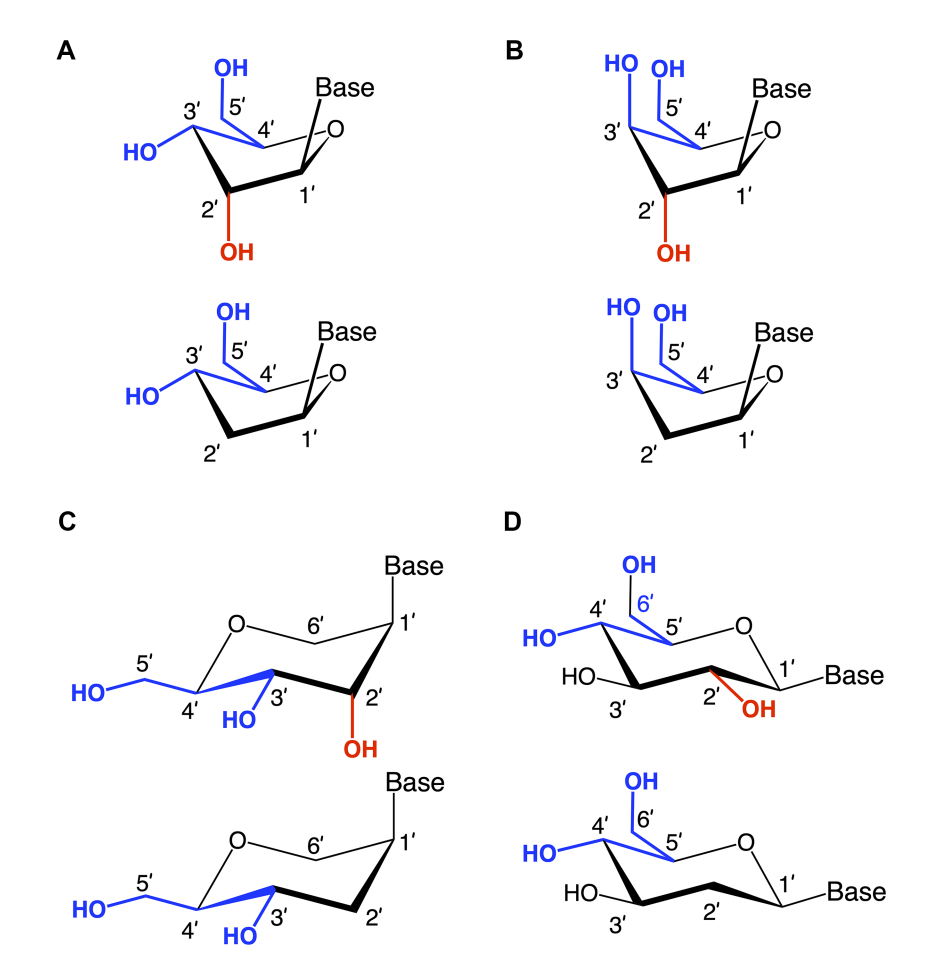


Figure 5. Nucleic acid pairing systems and their 2'-deoxy analogs. (**A**) RNA (top) and DNA (bottom), (**B**) XyloNA (top) and dXyloNA (bottom), (**C**) AltNA (top) and HNA (bottom), and (**D**) GlucoNA (top) and dGlucoNA (bottom). 2'-Hydroxyl groups are highlighted in red and backbone bonds are highlighted in blue  $(5'\rightarrow 3')$ , panels A-C, or  $(5'\rightarrow 4')$ , panel D).

nucleosides, were incorporated into Macugen (pegaptanib), a 27-mer RNA aptamer functioning as a VEGF antagonist [63]. More recently, Izervay, which shares 2'-F, 2'-OMe and PEG modifications with Macugen, received approval against complement protein C5 for treatment of geographic atrophy in the eye [64]. These chemical modifications enhance aptamer stability against endonucleases and influence its three-dimensional structure, which remains an area of active investigation.

### **Artificial genetic polymers**

Inspired by nature, chemists have spent the last 50 years systematically designing and synthesizing a vast array of sugar-modified nucleic acids. The entries provided in Table 1 were identified from the literature as genetic systems that collectively form what we now describe as the XNA alphabet. This table is limited to XNA systems that have been incorporated into oligonucleotides. Most have been the subject of limited

biochemical studies, which may include their influence on the thermal stability of a DNA or RNA duplex. Others have been synthesized as oligomeric XNA strands, and only in those cases has the full potential of the modification been revealed. Some of the more common examples of this series are FANA, TNA, HNA, ceNA, AltNA, tricyclicNA, LNA, homoDNA, pRNA, SNA, and aTNA, which have been evaluated in applications beyond simple recognition studies involving complementary Watson–Crick base pairing. We expect this table to grow overtime to include new examples, and we encourage members of the community to share their latest contributions with the co-authors of this review.

## Role of the sugar moiety in duplex formation

The sugar moiety of a nucleoside determines an oligonucleotide's conformation and hybridization properties. Various regio- and stereoisomers can arise in furanose nucleosides, and oligonucleotides derived from sugar-modified nucleosides exhibit distinct hybridization patterns. For example, in DNA, deoxyribose has a 1[R], 3[S], 4[R] configuration, enabling sequence-selective hybridization with both DNA and RNA with an antiparallel strand polarity. In contrast,  $\alpha$ -DNA, with a 1[S], 3[S], 4[R] configuration, hybridizes sequence-selectively with DNA but in a parallel strand orientation [154]. DNA can also form parallel duplexes with itself [155], but RNA duplexes are strictly antiparallel, a difference that has its origin in their distinct backbone-base inclinations (Fig. 2). In dXylo nucleic acids, where the sugar adopts a 1[R], 3[R], 4[R] configuration, DNA hybridization does not occur, making dXyloNA a fully orthogonal nucleic acid system that hybridizes exclusively with itself [58]. Similarly, 2'-5'-linked DNA features a sugar moiety in a 1[R], 2[R], 4[S] configuration, allowing RNA hybridization in an antiparallel strand orientation but not with DNA [156]. Interestingly, 2'-5'-RNA was found to bind to complementary ssRNA but only bind weakly, or not at all, to ssDNA [53, 157]. These findings underscore the view that sugar modifications, rather than base or phosphate modifications, are key to designing orthogonal XNAs.

#### Sugar pucker

This section provides an overview of the conformational properties of five-, six-, and seven-membered sugar rings. Sachse was the first to propose that the chair conformation eliminates strain in a planar cyclohexane ring [158]. A five-membered ring has two stable conformations—half-chair and envelope each with ten possible forms, as represented in the pseudorotational wheel of a five-membered ring. Kilpatrick [159] coined the term "pseudorotation" to describe the hypothetical motion of an out-of-plane atom around the ring (Fig. 6A). This motion is characterized by two coordinates: the ring puckering amplitude and the pseudorotational phase angle (P) [159]. However, when a five-membered ring is substituted, as in modified nucleosides, pseudorotation becomes restricted—a phenomenon described by Altona and Sundaralingam [160]. According to their pseudorotational wheel model, the C3'endo/C2'-exo twist conformation corresponds to  $P = 0^{\circ}$ (type N), while the C2'-endo/C3'-exo twist corresponds to  $P = 180^{\circ}$  (type S). Natural β-nucleosides primarily adopt Ntype or S-type conformations in dynamic equilibrium. Most conformationally restricted nucleosides described in the literature favor the N-type conformation, as it enhances hybridiza-

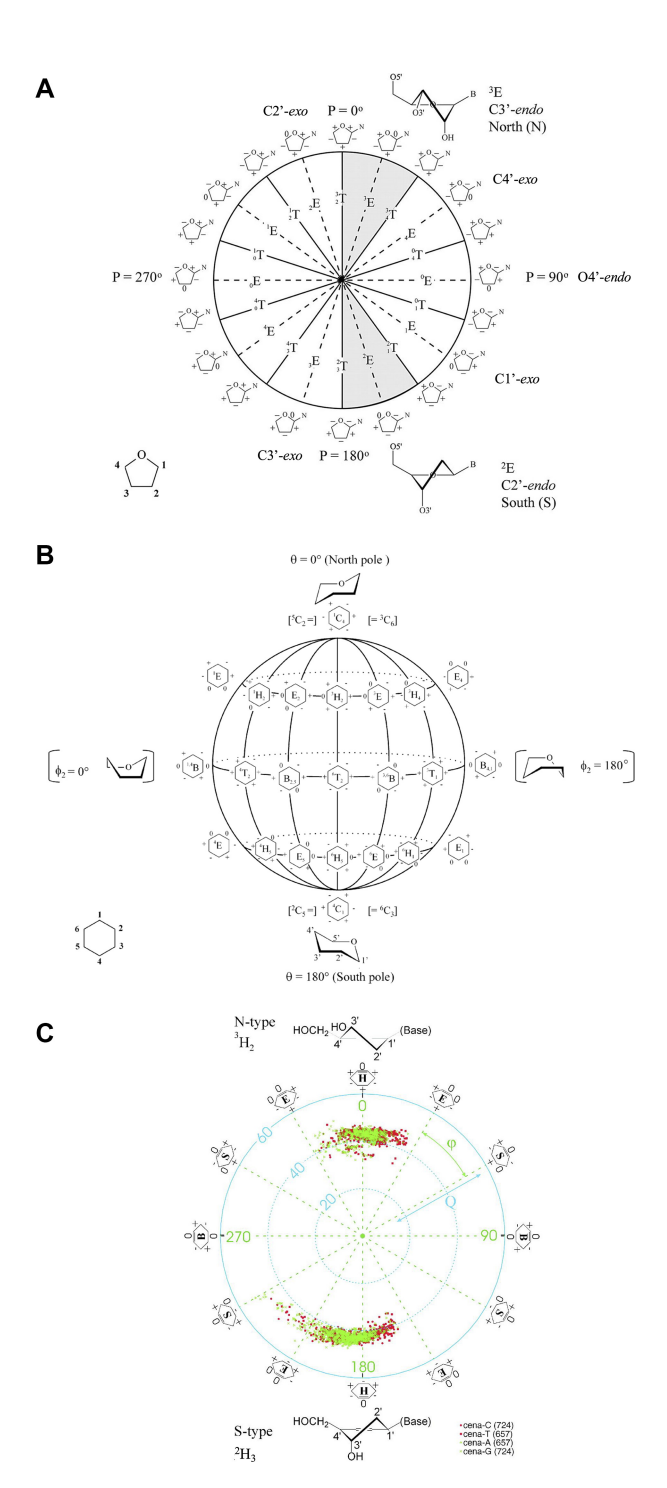


Figure 6. Conformational characterization of five-membered and six-membered (pyranose and cyclohexene) rings (A) Pseudorotation phase cycle of the furanose ring [173]. The preferred puckers of ribose and 2'-deoxyribose are shown at the top (N) and bottom (S), respectively. Points on the circle mark specific values of the pseudorotation angle P. Shaded regions represent conformations found in A- and B-form helices. Riboses on the periphery of the cycle indicate signs of the endocyclic torsion angles  $v_0$  to  $v_4$ : (+) positive, (-) negative and (0)  $0^{\circ}$ . (B) Pseudorotation globe of the cyclohexane ring [174]. The preferred conformations of pyranose are shown at the top (N) and at the bottom (S). Six-membered ring conformations are shown on the front surface of the globe with signs of the endocyclic torsion angles  $v_0$  to  $v_6$  indicated: (+) positive, (-) negative and (0) 0°. (C) Pseudorotational phase cycle of a cyclohexene ring [174]. Data points for 2775 randomly generated and energy-minimized structures of C, T, A, and G nucleotides (see color code at bottom right) are shown and demonstrate that the energetically most favorable conformations of the cyclohexene ring are of the <sup>3</sup>H<sub>2</sub> (N) and <sup>2</sup>H<sub>3</sub> (**S**) types. Reproduced with permission from [175, 176].

tion with RNA, which naturally adopts an N-type conformation in duplexes (Figs. 4, 6A). For example, TNA nucleosides adopt an N-type, C4'-exo conformation [29], explaining their preferential hybridization with RNA over DNA [41, 42]. In contrast, S-type sugar nucleoside analogs are rare, with examples including 3'- $\beta$ -Me-cordycepin [161] and  $\alpha$ -L-ribo-LNA nucleoside [128] (see Table 1 for structures). Others are AraNA (C1'-exo) [162] and  $\alpha$ -LNA (C3'-exo) [128]. By contrast, the FANA analog displays an East O4'-endo sugar pucker (Fig. 6A) [24].

Cremer and Pople defined ring puckering coordinates for six-membered rings, which predominantly adopt chair conformations [163]. Chair-chair interconversion occurs via boat and twist conformations, the three fundamental forms of a six-membered ring, alongside half-chair and envelope conformations. The conformational landscape of a six-membered ring is described by three parameters: the degree of puckering (q), the pseudorotational phase angle (P), and the total puckering amplitude (Q), with  $\Theta$  representing the degree of distortion (Fig. 6B). The two poles of the conformational globe correspond to the two chair conformations. The North pole represents the sugar conformation of HNA [28], which hybridizes with DNA and RNA, mimicking a natural nucleoside in the N-type conformation. The South pole corresponds to the sugar conformation of homo-DNA, which does not hybridize with DNA or RNA, making it an example of an orthogonal nucleic acid [164, 165]. Intermediate conformations, such as the 4',6'-methano and 1',6'methano carbocyclic nucleosides, have also been described [145, 166] (North and South methanocarba NA, respectively, Table 1). These adopt boat-like conformations near the equatorial plane of the conformational globe. The 4',6'methano nucleoside mimics a furanose nucleoside in its C2'exo conformation, stabilizing DNA/RNA duplexes, while the 1',6'-methano nucleoside mimics a furanose nucleoside in its C3'-exo conformation, destabilizing them. As observed in furanose-type nucleosides, pyranose-type nucleosides also exhibit hybridization properties dictated by sugar substitution and conformation, enabling orthogonality in both sugar types.

Cyclohexene rings present a unique case, as their two sp²-hybridized carbon atoms restrict conformational flexibility. Consequently, cyclohexene rings tend to be locked in energy minima along an elliptical trajectory of boat and half-chair forms, similar to five-membered rings. The  $^2H_3$  conformation of a cyclohexenyl nucleoside mimics a C2'-endo furanose nucleoside, while the  $^3H_2$  conformation resembles a C3'-endo furanose nucleoside, with a low interconversion energy barrier [167] (Fig. 6C). The  $^3H_2$  conformation is stabilized by a  $\pi$ – $\sigma$ \* interaction, motivating the synthesis of cyclohexenyl nucleic acids (CeNA, Table 1), which hybridize with both DNA and RNA [87]. X-ray structures of CeNA/DNA hybrids reveal the coexistence of both half-chair conformations [168].

Oligonucleotides with 7'-5' linked seven-membered sugar rings, such as oxacycloheptane (oxepane, OxNA, Table 1), have also been synthesized and tested for heteroduplex formation with DNA (oT15:dA15) and RNA (oT15:rA15), as well as their ability to elicit RNase H cleavage of RNA strands in hybrids [138]. The seven-membered ring is expected to be more flexible than five- or six-membered rings, adopting conformations such as chair, twist-chair, boat, twist-boat, and intermediate forms [169]. Theoretically, twist-chair conformers are energetically favored due to minimal steric interactions

[170]. A crystal structure of oxepane confirmed its twist-chair conformation [171]. However, applying Cremer and Pople's four ring-puckering parameters (q2, q3, Φ2, and Φ3) [50] to the oxepane crystal structure showed that its conformation is best described as an intermediate between twist-chair and twist-boat [171]. Subsequent studies of oligonucleotides containing oxepane-thymidine revealed significant differences in pairing behavior and stability depending on backbone connectivity, including 7′-5′ (OxT0), 7′-5′ with 4′ and 3′ hydroxy groups (OxT1), 7′-4′ with 5′ and 3′ hydroxy groups (OxT2), and 7′-3′ with 5′ and 4′ hydroxy groups (OxT3) [172]. Molecular dynamics simulations indicated that each oxepane variant exhibits distinct conformational preferences, with varying degrees of twist-chair occurrence.

### Backbone inclination angle

Nucleic acid structural parameters can be categorized into those that define the local geometry of base pairs and those that impact the geometry of the helix [177]. The latter are particularly crucial for assessing structural orthogonality and the potential for self- and cross-pairing of XNAs. Among these, the inclination angle ( $\eta$ ) quantifies the relative orientation of the base pairs with respect to the global helical axis. The backbone-base inclination angle ( $\eta_B$ ) is specifically defined as the relative orientation between the normal of the base or base pair and the BSpline backbone curve, which is traced by the phosphorus atoms of an oligonucleotide strand as it intersects the base plane [178] (Fig. 2).

While B-form DNA inherently lacks backbone-base inclination, A-form duplexes (both DNA and RNA) exhibit inclination angles exceeding -30° (Fig. 2). The extent of inclination in XNAs is particularly evident in low-twist pairing systems (Fig. 7), such as homo-DNA ( $\eta_B = +35^\circ$ ) [15, 164] and pRNA ( $\eta_B = -46^\circ$ ) [30]. Increasing backbone-base inclination in XNAs enhances selective hybridization—favoring selfpairing over cross-pairing with DNA/RNA—and contributes to duplex stability through interstrand stacking, acting as a form of molecular glue (Fig. 8). Similarly, reducing helical twist (which in turn increases base pair rise) promotes selective hybridization and structural orthogonality (Fig. 7). The helical twist angle is primarily determined by the  $\delta$  angle of the sugar moiety (e.g. ribose or 2'-deoxyribose, Figs. 1 and 4) and the phosphate geometry. The feasibility of achieving orthogonality depends on the intricate interplay between inclination and twist parameters and their capacity to establish an XNA geometry that is inherently distinct from dsDNA and dsRNA (Fig. 8).

### **Duplex geometries**

### Self-pairing versus cross-pairing

Most XNAs described to date are self-pairing systems, forming antiparallel duplexes that are governed by standard Watson–Crick base pairing rules. Cross-pairing between different XNAs or between XNAs and RNA or DNA only occurs when their helical geometries share similar inclination angles and twist parameters. Table 2 presents these parameters for XNAs that cross-pair with RNA, derived from X-ray structures or, when unavailable, NMR studies. Notably, the twist and inclination values for these dsXNAs closely resemble those of dsDNA and dsRNA (e.g. (S)-GNA and TNA Fig. 9A,B), with the exception of dsHNA (structure 2), which

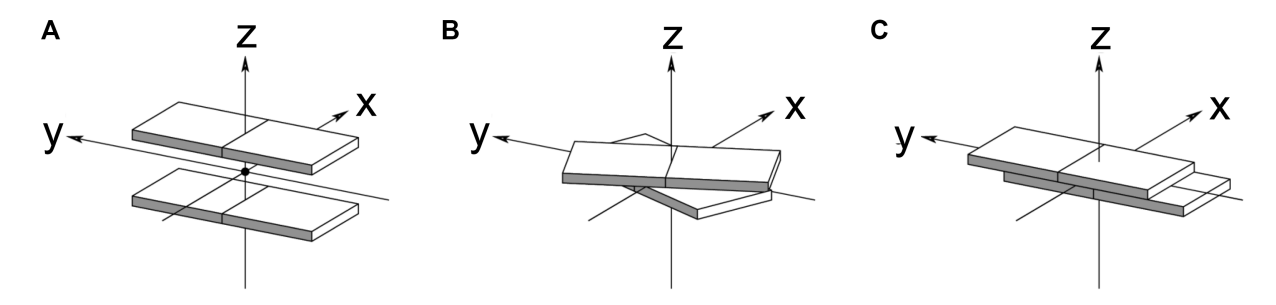


Figure 7. Definition of nucleic acid helical structural parameters (A) rise, (B) twist, and (C) slide [2]. Illustrations adapted from [3, 179].

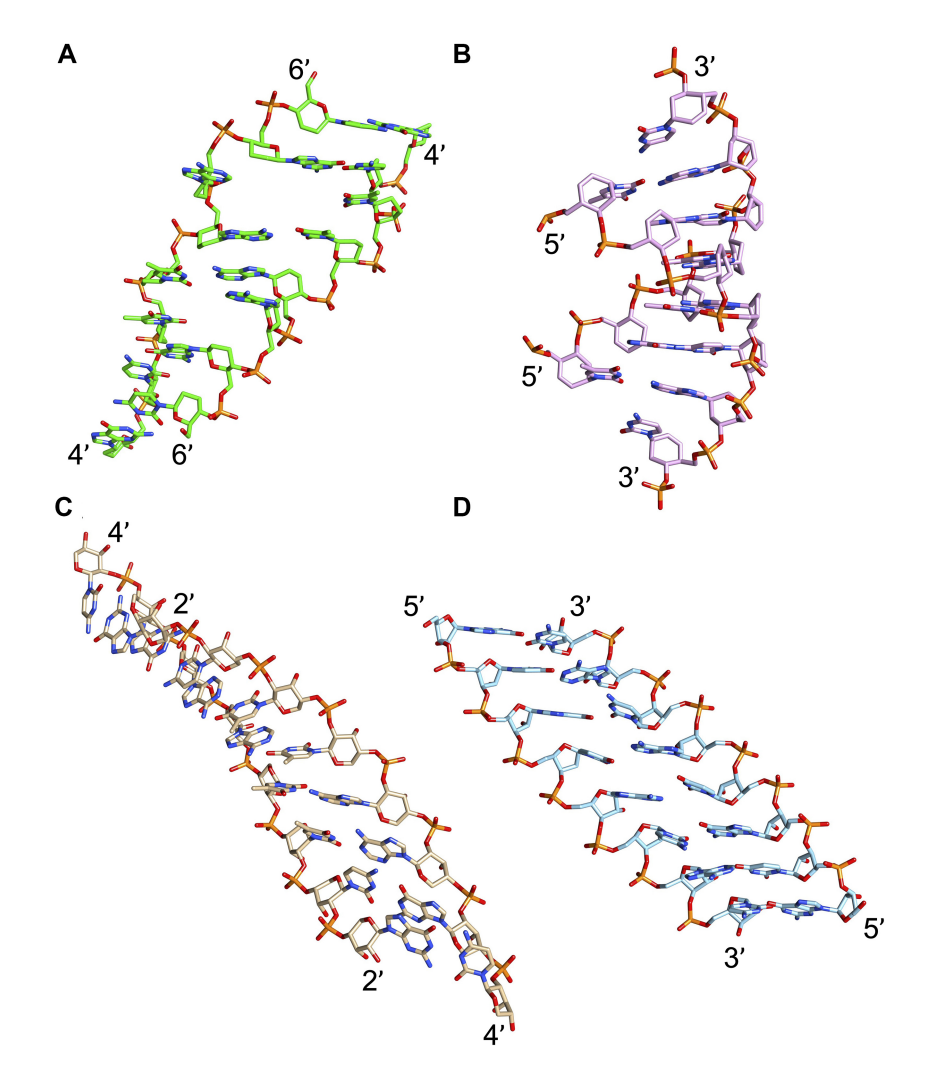


Figure 8. Structural models of orthogonal XNA pairing systems that display low helical twist and concomitant enhanced slide and interstrand stacking (homo-DNA, pRNA, XyloNA) or are left-handed (L-CeNA). (A) homo-DNA 6'-dd(CGAATTCG)-4', X-ray structure, PDB ID 2H9S [164]. (B) L-CeNA 5'-c(GTGTACAC)-3', X-ray structure, PDB ID 2H0N [180]. (C) pRNA 4'-p(CGAATTCG)-2', NMR solution structure [181]. (D) XyloNA 5'-x(GUGUACAC)-3', NMR solution structure, PDB ID 2N4J [31].

Table 2. Helical twist and inclination angles for selected XNAs that cross-pair with RNA

XNA Reference	dsHNA 1 [182]	dsHNA 2 [164]	HNA:RNA* [183]	CeNA:RNA [184]	AltNA:RNA [185]	dsTNA [43]	P <sup>N</sup> DN [47]
Method	X-ray	X-ray	X-ray	X-ray	X-ray	NMR	X-ray
Twist [°]	33.2	24.2	31.5	31.3	30	27.4	33.2
Inclination [°]	24.3	3.4	14	17.1	13.7	24.1	14.7

<sup>\*</sup>Average of four different structures

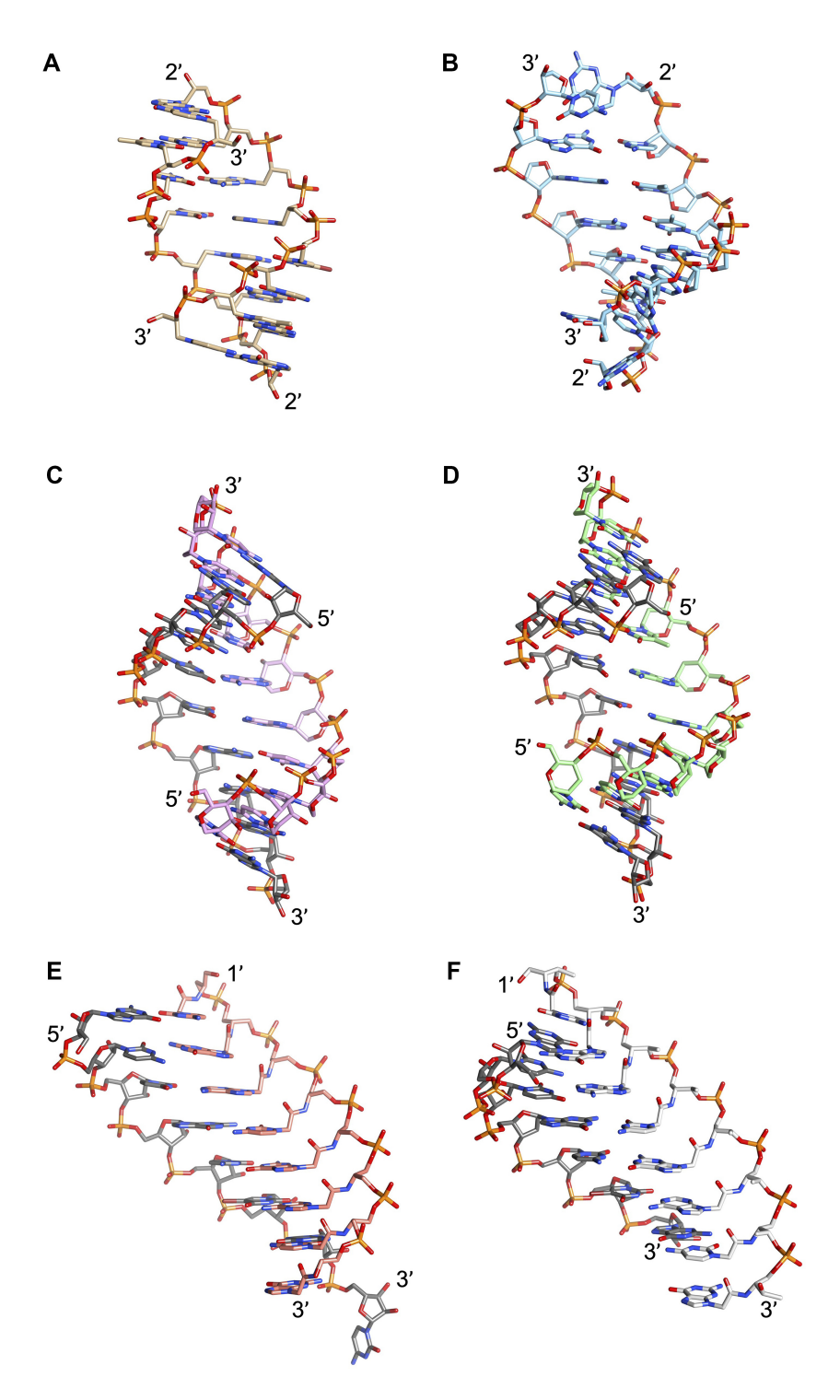


Figure 9. Structures of XNAs that cross-pair with RNA. (A) (S)-dsGNA 3'-g(CTC(Br)UAGAG)-2', X-ray structure, PDB ID 2XC6 [187]; note that the C5-methyl group of T points into the minor groove as (S)-GNA adopts a right-handed duplex conformation with an inverted orientation of base pairs like in Z-DNA. (B) dsTNA 3'-t(CGAATTCG)-2', NMR solution structure [43]. (C) AltNA:RNA 5'-alt(CCGUAAUGCC-P)-3': 5'-r(GGCAUUACGG)-3', X-ray structure, PDB ID 3OK2 [185]. (D) HNA:RNA 5'-h(CCGTAATGCC)-3': 5'-r(GGCAUUACGG)-3', X-ray structure, PDB ID 2BJ6 [183]. (E) SNA:RNA 3'-s(GCAGCAGC)-1': 5'-r(GCUGC(Br)UGC)-3', X-ray structure, PDB ID 7BPF [192]. Carbon atoms of RNA strands are colored in gray.

exhibits reduced helical twist, minimal inclination, and a slightly unwound duplex (15 base pairs per turn). This demonstrates that even conformationally restricted XNAs retain some structural malleability.

A second class of XNAs includes those with low twist values, such as dsPNA (~19° twist, yielding 18 base pairs per turn, a configuration unattainable in DNA or RNA) or large inclination angles, as seen in dsGNA (Table 3). Despite such deviations, these XNAs can still cross-pair with RNA due to their acyclic, flexible backbones, as demonstrated in dsGNA structures [186] (Fig. 9A). Interestingly, dsGNA exhibits negative inclination similar to RNA and the (*S*)-isomer of GNA hybridizes with RNA, but is unable to pair with DNA (no inclination, Fig. 2A) or homo-DNA that exhibits a strongly positive inclination (Fig. 8A). The structural differences between dsPNA and PNA:RNA hybrids further highlight the adaptability of PNA.

Table 4 offers examples of orthogonal XNAs that do not hybridize with RNA or DNA. From these data, it is evident that significant deviations in either twist or inclination preclude cross-pairing. Another key determinant is backbone flexibility: XNAs with non-acyclic sugar moieties exhibit limited rotation around one or more backbone angles, affecting their ability to hybridize. For instance, pentopyranose (4'-2') oligonucleotides possess two fixed backbone angles, while pentofuranose (5'-3') nucleic acids retain one backbone angle with restricted rotation, making the latter more conformationally adaptable.

The significance of inclination in hybridization was experimentally demonstrated by Eschenmoser and collaborators. The pentopyranosyl (4'-2') oligonucleotide family exemplifies strongly self-pairing systems that cross-pair within their class but not with RNA [193]. Cross-pairing occurs only between nucleic acids with similar geometries. For example, pentopyranose nucleic acids ( $\beta$ -D-ribo,  $\alpha$ -L-arabino,  $\beta$ -D-xylo, and  $\alpha$ -L-lyxo) are predicted to adopt quasi-linear double strands with antiparallel strand orientation, comparable twist, and inclination [84]. However, despite their structural similarity, they are unlikely to cross-pair in an antiparallel duplex with homo-DNA due to the opposite sign of backbone inclination [4, 193, 194] (Fig. 8).

### Orthogonal nucleic acid pairing systems

Synthetic biology aims to design and create new living systems with useful applications in medicine, agriculture, and material sciences. To ensure that these synthetic systems do not interfere with natural ecosystems, their genetic information should be encoded in artificial nucleic acids that cannot communicate with DNA and RNA [195]. A coding strategy of this type would prevent unintended genetic exchange with the natural genetic information of the cell. Additionally, polymerases (Pols) used to synthesize orthogonal XNAs must not interfere with the natural replication of DNA and RNA. By using orthogonal XNAs, synthetic biology can achieve a higher level of safety [196].

In this context, orthogonality refers to the inability of artificial nucleic acids to exchange genetic information with DNA or RNA, meaning they can only pair with themselves. DNA and RNA adopt specific helical conformations, primarily A-and B-form structures. Modifying the sugar component of a nucleic acid can produce XNAs with duplex geometries that

**Table 3.** Helical twist and inclination angles for selected XNAs with low twist and/or large inclination that still cross-pair with RNA

XNA Reference	dsGNA [187]	dsPNA [188]	PNA:RNA [189]
Method	X-ray	X-ray	X-ray
Twist [°]	22.9	19	26
Inclination [°]	-46	3	14

fall outside the conformational space occupied by natural nucleic acids (Fig. 8).

The key structural parameters that determine orthogonality are inclination (slide) and twist [197] (Fig. 7). These factors influence rise, which affects the stacking distance between nucleobases. For example, D-DNA and L-DNA are mutually orthogonal [198] because they have the same inclination but opposite twist—D-DNA is right-handed, while L-DNA is left handed. However, as seen with dsGNA, XNAs can exhibit structural flexibility, meaning that simply analyzing the geometry of a self-complementary duplex is not enough to determine orthogonality [187].

To confirm whether an XNA is orthogonal to natural nucleic acids, hybridization studies should be performed using XNA oligonucleotides with all four nucleobases (mixed sequences). Relying only on polyA:polyT hybrids can lead to incorrect conclusions, as demonstrated with L-DNA [198].

#### Helical versus linear

The twist angle  $(\Omega)$  is the parameter that determines the helicity of a double-stranded helix, while the repeat refers to the number of base pairs per helical turn. The twist angle represents the rotation of base pairs around the helical axis and can be positive (right-handed) or negative (left-handed) (Fig. 7B). However, it is not uniform along the helix—it varies depending on the nucleotide sequence [199]. This issue is less important in the context of the discussion about orthogonality, and we will use average values to describe the helicity of a double stranded helix. For example, a helical structure with 10 base pairs per turn and a rise of 3.4 Å (resulting in a pitch of 34 Å) will become a fully linear structure with an infinite number of base pairs per turn if completely unwound. As the helix unwinds, the base pair rise (Fig. 7A) increases. Because of this, nucleic acids with significantly different twist angles cannot hybridize with each other. Fig. 10 illustrates XNAs with twist angles ranging from  $+36^{\circ}$  to  $-36^{\circ}$  [175, 198] (see Table 1 for structures).

The dsXNAs provided in Table 2 reside on the left (West) side of the x-axis, indicating they cross-pair with DNA and/or RNA. One exception could be the  $\alpha$ -homo-DNA:RNA duplex, which has a twist angle of  $26.2^{\circ}$  and an inclination of -1.78 Å. However, similar to  $\alpha$ -DNA, it hybridizes with RNA in a parallel orientation, which complicates replication [197]. Aside from L-nucleic acids, promising candidates for an orthogonal genetic system include aPhoNA (dsZNA) [65], pRNA [181], and dXylo nucleic acids [58], which reside in the center or right (East) side of Fig. 10. Studies have shown that some Pols—such as Klenow exo- and Pol  $\beta$  SP20 can recognize modified nucleoside triphosphates as substrates, though only to a limited extent. Additionally, a trimer (one codon) has been successfully transliterated into DNA in  $E.\ coli\ [200]$ . However, to fully synthesize an XNA gene  $in\ vivo$ , it will be necessary

Table 4. Helical twist and inclination angles of selected XNAs that do not cross-pair with DNA/RNA

XNA Reference	ds-L-RNA [190]	ds-L-CeNA [180]	ds-homo-DNA [164]	ds-apNA [191]	ds-pRNA [181]	ds-dXyloNA# [58]	ds-XyloNA [31]
Method	X-ray	X-ray	X-ray	NMR	NMR	NMR	NMR
Twist [°]	-31.0	-29.6	14.3	small*	19	3.1	10.7
Inclination [°]	14.3	12.7	44.2 $(\eta_{\rm B})$	-50	$\sim$ -40	-50.6	-45.2

<sup>\*</sup>No significant helicity, although NMR experimental restraints do not define this parameter directly due to their short-range nature (coordinates not available). #Average value of two different structures.

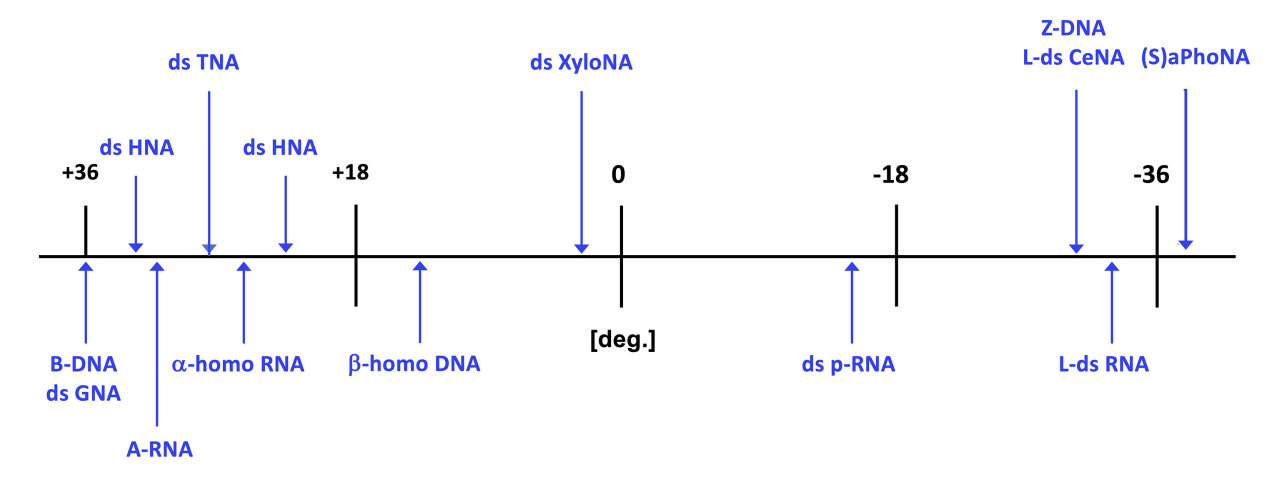


Figure 10. Average helical twist values (rotation/base pair in degrees) for DNA/RNA and selected XNAs.

to evolve mesophilic Pols capable of enzymatic XNA synthesis. So far, the complete chemical synthesis and expression of a fully modified gene in *E. coli* has only been demonstrated for base-modified oligonucleotides [201]. This finding raises new questions about the structural flexibility of dsXNAs, the role of hydration in duplex stabilization, and the polymerization process [202]. Because some flexibility is needed for Pols to evolve and support XNA synthesis, dXyloNA (Fig. 5) may be a better candidate for an artificial genetic system than pRNA (which is too rigid, Fig. 8) or ZNA (which is too flexible) [203].

### Role of chirality

The twist angle (and thus the helicity) is also an important factor determining hybridization between oligonucleotides of opposite chirality. For example, β-D-homo-DNA (polyA), with three stereogenic centers per nucleotide, forms heterochiral duplexes with  $\beta$ -L-homo-DNA (polyT) whereby the duplex is more stable than the homochiral system [204]. This heterochiral duplex displays virtually no twist and a strong backbone inclination as demonstrated using molecular modeling. β-D-Homo-DNA (polyA) also forms very stable duplexes with L-HNA (polyT) [114], most probably because HNA can also adopt a ladder-like conformation with equatorial orientation of bases and thus a duplex with low twist values [205]. Conversely, single-stranded GNA, with only one stereogenic center per nucleotide, is preorganized into a helical structure [206]. Like DNA and RNA strands of opposite chirality, (S)-GNA and (R)-GNA do not base pair with each other [110], because the single stranded oligomers feature an opposite helical twist. In this case, a mixed A/T sequence was studied. Thus, exchange of information between two homochiral oligomers of opposite chirality is a matter of their geometry, rather than of the type or numbers of their stereogenic centers.

PNA is achiral and can hybridize with both L-DNA and D-DNA [207]. Consequently, PNA can serve as a template for nonenzymatic L-RNA synthesis, representing an interesting case of informational transfer between two different XNAs [208]. SNA becomes chiral only upon incorporation into an oligonucleotide [209]. As a result, its chirality is sequence-dependent, with palindromic sequences remaining achiral. This also enables the same SNA sequence to hybridize with both D-DNA and L-DNA but in opposite orientations ( $5' \rightarrow 3'$  and  $3' \rightarrow 5'$ ). However, enantiomeric oligonucleotide hybridization can become complex when the XNA exhibits extensive conformational diversity. For instance, D-cyclohexane nucleic acid hybridizes with D-DNA, whereas L-cyclohexane nucleic acid hybridizes with D-homoDNA, forming duplexes with distinct geometries [210].

### **Biophysical properties**

The stability of nucleic acid structures depends on various factors, such as sequence, H-bonding, stacking interactions, hydration, counter ions, preorganization of single-stranded (ss) oligonucleotides, and crowding conditions. Additionally, the thermodynamic behavior of nucleic acids is influenced by the out-of-equilibrium conditions that persist inside cells. These factors also affect the ability of nucleic acids to recognize Watson-Crick base pairs or mismatched pairs like wobble or Hoogsteen base pairing modes. While these topics have been covered extensively in previous reviews, this section will focus on a few key examples from the XNA field (Table 1).

#### Example 1: Conformational preorganization

XNAs with rigid backbone structures are more preorganized as single strands than XNAs with more flexible backbones, which gives them an advantage in forming stable double-

stranded structures. Studies on HNA and AltNA compared to RNA and Mannitol Nucleic Acid (MNA) show that ssHNA and ssAltNA are preorganized into A-type structures (Fig. 9C and D), which are more stable than ssRNA [133]. This preorganization helps form more stable duplexes, including selfcomplementary XNA and RNA:XNA hybrids. MNA, on the other hand, adopts a conformation different from A- and Bforms, making it less effective at hybridizing with RNA [211]. Frequent H-bonds between the 3'-hydroxyl and the 6'-O of the phosphate backbone of the following base changed the conformation of the single strand as well as the MNA:RNA complex. The MNA:RNA backbone widens up and shows partial unwinding and disruption of base pair H-bonds consistent with their low hybridization potential. To achieve a higher state of preorganization, the sugar moiety of XNAs can be designed with bicyclic [20] or tricyclic sugar [212] structures or the ribose sugar can be modified to favor a C3'-endo conformation. This can involve substituting electronegative groups, like fluorine in the 2'-position or less electronegative groups like NH in the 3′ position [44].

Intrastrand stacking contributes significantly to nucleic acid stability by further organizing the backbone in a single stranded state. This stacking stabilizes duplexes that display C3'-endo sugar puckering. XNAs such as XyloNA [31] and pRNA [4] benefit from this type of stabilization. Acyclic nucleic acids generally do not hybridize well with DNA or RNA [209]. One exception is (S)-GNA, which can hybridize with RNA under certain conditions [213, 214]. Similar exceptions include PNA [25] and SNA [209] (Fig. 9E). PNA is especially notable for its ability to pair with both D- and L-DNA and RNA [207]. (S)-ZNA, another acyclic nucleic acid, can form stable self-complementary duplexes but hybridizes poorly with DNA. This behavior is partly due to the compactness of the ZNA structure. The reduced hybridization ability of (S)-GNA with DNA is attributed to the inverted orientation of GNA bases, which reduces H-bond formation with G:C pairs [214, 215].

Introducing chemical groups that restrict conformational flexibility, such as amido groups, can enhance hybridization between acyclic nucleic acids and DNA or RNA. For example, introducing a methyl group into the backbone of SNA produces threoninol nucleic acid (aTNA) [216] (Fig. 9F). This chemical modification increased duplex stability with DNA and RNA, especially for the L-isomer (L-aTNA), while the D-isomer (D-aTNA) is orthogonal to DNA and RNA [192, 216].

The preorganization of nucleic acids is also influenced by the phosphate in the backbone. The presence of certain conformations, such as gauche-trans and trans-trans orientations, impact free energy [217]. Introducing methylene phosphonate groups into the backbone increases flexibility [218] and changes sugar puckering [219]. Preorganization can also affect the susceptibility of nucleic acids to degradation by nucleases. Phosphodiesterases cleave a P-O bond in nucleic acids by an addition-elimination mechanism via the formation of a penta-covalent intermediate that generally collapses into 5'phosphorylated fragments. The nucleophiles involved in this reaction can be diverse and range from water to protein side chains like Tyr, Ser, and His [220]. Nucleases can be specific for DNA or RNA or be nonspecific [221]. Nothing is known about the substrate specificity of nonspecific nucleases, and it is unclear whether such enzymes are capable of also degrading certain XNAs. Examples of sugar non-specific endonucleases are staphylococcal nuclease from S. aureus [222] and rat liver nuclease [223]. Most DNases are metal ion dependent nucleases and cleave nucleic acids in the base-stacked helical conformation [220]. Conformational preorganization of the single strand may help in binding of the nucleic acids to the enzyme and their absence may contribute to the enzymatic stability of acyclic nucleic acids. It is generally accepted that the most relevant nucleases in the context of therapeutic oligonucleotides are 3'-exonucleases, and as such, phosphorothioate [214, 224], 3'-terminal XNAs [225], and inverted 3'-3' linkages [226] can stabilize the oligonucleotide against nucleolytic degradation.

### Example 2: Mismatch discrimination

Exchanging the 2'-deoxyribose sugar in DNA for a 2',3'dideoxyglucose sugar, such as the one found in homo-DNA results in altered base pairing priorities despite both systems having standard A, C, G and T nucleobases in both systems:  $G:C > A:T (DNA) \text{ versus } G:C > A:A \approx G:G > A:T > A:C$ (homo-DNA) [227]. The purine-purine (Pu:Pu) pairs in homo-DNA are of the reverse-Hoogsteen type. Thus, if one generated a very long homo-DNA of random sequence and the molecule adopted a folded state, it is very likely that there would be many reverse-Hoogsteen Pu-Pu pairs in addition to standard G:C and A:T pairs. In fact, it was found in the crystal structure of the homo-DNA octamer dd(CGAATTCG) [164] that one of the As is looped out of the duplex (Fig. 8A) and forms a reverse-Hoogsteen pair after it is inserted into the adjacent duplex opposite an orphaned T [178]. The other A forms an intermolecular reverse-Hoogsteen pair with T from the adjacent duplex. In the crystal the homo-DNA octamer engages in a dimer of dimers and there are multiple G:G pairs in the lattice. Consequently, the term mismatch is relative and somewhat dependent on the chemistry of the nucleic acid backbone.

Natural genetic polymers, especially RNA, can adopt a diverse range of base pair orientations [5]. Whenever RNA is being encoded (transcription) or decoded (translation), or in telomerase (guide), the spliceosome, the signal recognition particle, etc., the molecular machines doing the job have to keep RNA in a more-or-less canonically paired duplex state. If RNA were to adopt a complex 3D fold it needs to be unwound and reigned in as the fold is choked full of non-Watson-Crick pairs. Hence there must have been evolutionary pressure to transition to DNA for storing the genetic information as RNA is much too promiscuous in terms of pairing and stacking whereas DNA is faithful and monotonous by comparison.

A biologically relevant mismatch base pair is the G:U wobble pair in RNA. It serves many RNA functions such as in tRNA aminoacylation and ribosomal activity, splicing and ribozyme activity [228]. However, at the level of DNA wobble base pairing is unwanted as it leads to mutagenesis. A G:U wobble pair leads to a local structural perturbation of dsRNA. The glycosidic bond angle at C1' of the ribose sugar of W-C base pairs is  $\sim 55^{\circ}$ . In a G:U wobble pair these values are  $\sim$ 40° for G, and  $\sim$ 70° for U [228]. This leads to undertwisting and overtwisting, respectively, of the helix at the wobble position [229]. Therefore, one would expect that in conformationally more rigid XNA structures, mismatch discrimination will be higher and the fidelity of base pairing increased as less conformational dynamics will be allowed. Although this was only studied in an 8-mer duplex (which may cause large differences in T<sub>m</sub> values dependent on the localization of the

**Table 5.** Recognition of isoC<sup>Me</sup> and isoG bases on DNA and HNA templates in insertion assays under different conditions using Klenow Fragment (-) as Pol. The substrates tested are dCTP, dTTP, dGTP, and dATP. The table only lists the nucleotide triphosphate that is most efficiently incorporated opposite the modified base

Template	In vitro conditions	Crowding conditions	In vivo (E. coli)
isoC <sup>Me</sup> in DNA	dATP	dATP	dGTP
isoG in DNA	dTTP	dTTP	dTTP
isoC <sup>Me</sup> in HNA	dGTP	dGTP	dGTP
isoG in HNA	dCTP	dCTP	dTTP

mismatch base pair in the duplex and the neighboring base effects), the  $\Delta T_m$  values for mismatch discrimination were higher in the HNA:RNA duplex relative to the RNA:RNA duplex [230]. The  $\Delta T_m$  between match and mismatch base pairs in the RNA:HNA duplex varied between –12.8° (C:A mismatch) and –38.2° (G:A mismatch). In the RNA:RNA duplex, the values varied between –3.9° (G:U mismatch) and –27.9° (G:A mismatch). Thus, the G:U wobble pair in dsRNA leads to a  $\Delta T_m$  of –3.9°. Although the data cannot be strictly compared because in the HNA sequence U was replaced by T, the  $\Delta T_m$  of the G(RNA):T(HNA) mismatch was –12.9°. In the reversed pair (G in HNA and U in RNA) the difference in  $\Delta T_m$  was much lower, i.e. –1° in favor of HNA:RNA.

These preliminary limited data point to the possibility that the use of conformationally restricted XNAs as genetic polymers might produce increased fidelity of base pairing. When considering applications in synthetic biology, an important question is how the XNA sugar will influence base pairing "in vivo." The intracellular environment is a gel-like matrix [231] and different from the conditions that are used for DNA Pol-catalyzed nucleotide incorporation assays in vitro. Initial studies have been performed using crowding conditions "ex vivo" [232] and using an 'in vivo' model in E. coli [233] with isoCMe and isoG bases on DNA and HNA templates. This means that mismatch recognition is evaluated and not matched recognition as it is expected that isoC preferentially base pairs with isoG; in the in vivo assay only pairing with A, C, T, and G can be evaluated. The E. coli DNA Pol I Klenow fragment was used as surrogate enzyme in the in vitro assays and the difference in recognition pattern is sometimes small. For example, under crowding conditions and using Klenow fragment, CTP and dTTP were incorporated in almost equal quantities opposite the isoG base on an HNA template [232]. In Table 5, only the nucleoside triphosphate most efficiently incorporated is mentioned, independent of the difference relative to other NTPs. The data demonstrate that using PEG200 as the crowding agent does not allow perfect mimicry of in vivo conditions and results will likely deviate from those "in vivo." In the present case, the selectivity of in vivo recognition of isoCMe and isoG on a DNA template is the same as on an HNA template.

#### Example 3: Hydration

The role of water in stabilizing nucleic acid structures has been well documented [234]. High humidity favors the B-form and low humidity favors the A-form [235]. The major groove is more hydrated than the minor groove and the water structure entails primary and secondary water layers [236, 237]. Water molecules in the primary layer exhibit a high residence

time and this layer behaves as quasi crystalline water [238]. This also means that Watson–Crick base-pairing is additionally stabilized by H-bonding due to hydration. A G:C base pair involves three Watson–Crick H-bonds and is further stabilized by 8 water molecules in the grooves. In an A:U base pair, there are two Watson–Crick H-bonds and five water molecules in the grooves [239]. Clearly, water is a factor that should be considered when base-modified nucleic acids are evaluated in synthetic biology. The introduction of 7-deazapurine bases, for example, leads to dehydration of the major groove, thereby triggering increased conformational plasticity of the modified nucleic acids [202], which results in a change of the fidelity of base pairing [240].

#### Example 4: Charge repulsion

Electrostatic repulsion between phosphate groups in nucleic acids is minimized by counter ions, such as divalent ions, which are more effective than monovalent ions like Na<sup>+</sup>. This repulsion can also be reduced by using XNAs with a neutral backbone, such as PNA, which hybridizes with DNA and RNA independently of ionic strength. The neutral backbone of PNA makes it a strong probe for strand displacement and for forming stable triplexes [188], though it has limited cellular uptake [241], which restricts its use in synthetic biology applications. Nonetheless, PNA remains a valuable tool for diagnostic purposes [242].

### Synthesis, replication, and evolution

The events that led to the origin and evolution of life on Earth rely on several key biological processes that include the diversification, replication, and propagation of genetic information in actively dividing cells. Since evolution occurs at the cellular level, genes that increased the fecundity of a cell were retained by natural selection, while those with deleterious properties were lost to extinction. As cells continued to grow and divide, protein secondary and tertiary structures are thought to have emerged as genetic sequences recombined in various ways to produce new types of proteins, including those with novel folds and functions [243-246]. The key biochemical reaction for replication is phosphodiester bond formation. In this reaction, the growing strand is recognized as a primer that is extended in the 5'-3' direction by sequentially adding 5'-nucleoside triphosphates to the terminal 3'-hydroxyl group as dictated by the sequence of the complementary template [247]. Recombination is a more complex process that involves the biochemical steps of transesterification, phosphodiester hydrolysis, and intermolecular ligation, which allow segments of DNA and RNA to be shuffled or removed, as is the case for RNA splicing [248].

Some RNA splicing events catalyzed by ribozymes can also be performed by DNAzymes. Early examples included DNAzymes that cleave and ligate RNA substrates at specific nucleotide positions [249, 250]. When first discovered, these results demonstrated that DNA molecules, like RNA before it [251], have the capacity to fold into shapes with catalytic activity. Growth in this area led to the discovery of second-generation DNAzymes that function under simulated physiological conditions and can achieve persistent allelespecific gene knockdown activity of endogenous mRNAs in cells [252–254]. This approach relies on the unique physicochemical properties of XNAs to increase catalytic activity

and biostability of the DNA scaffold. Engineered Pols have extended the types of genetic polymers that are capable of enzymatic catalysis to include a small but growing set of XNAs, like TNA, HNA, and FANA, that can be evolved in the laboratory to cleave and ligate RNA substrates [252, 255–257]. Expanding these systems to include the evolution of XNAzymes that can act on XNA substrates is an important area of future growth.

Nucleic acid biochemists have long appreciated the importance of the 2' hydroxyl group on the ribose sugar as a reaction moiety for RNA transesterification. For example, all RNA-cleaving nucleic acid enzymes follow the same metaldependent reaction mechanism to produce an upstream cleavage product carrying a 2',3'-cyclic monophosphate and a downstream strand with a 5' hydroxyl group. This reaction involves nucleophilic attack of a 2' oxyanion on the neighboring phosphodiester bond, which can only be achieved by the deprotonation of a vicinal diol, like the one found on RNA. This unique mechanistic feature implies that only XNAs with vicinal diols are capable of recombination using ribozymes to cut and ligate RNA segments together. This hypothesis proved correct for altritol nucleic acid (AltNA, Fig. 5C) in a nonenzymatic reaction format that identified the *cis*-diol configuration shared by RNA as a fundamental determinant of hydrolysis [57]. This finding suggests that XNAs with a cis-diol on their sugar moiety are important model systems for prebiotic chemistry and possible RNA progenitor candidates for the evolution of life.

Nonenzymatic polymerization and ligation reactions have long served as a model for RNA synthesis in the absence of complicated enzymatic machinery [258]. These reactions follow a mechanism in which the 3'-hydroxyl group attacks a 5'activated monophosphate on the incoming mononucleotide, or the case of ligation, a 5'-activated oligonucleotide. Leaving groups used to achieve phosphodiester bond formation include 2-methylimidazole [259], 2-aminoimidazole [260], oxyazabenzotriazole [261], and proline [262]. The nonenzymatic transfer of genetic information from RNA templates to XNA products have been demonstrated for a number of systems, including PNA [263], p-RNA [264], TNA [265–267], and MNA [268]. Likewise, HNA [269], AtNA [270], GNA [271], and TNA [272] offer examples of XNA templates examined for RNA transcription. Nonenzymatic replication within the same XNA system has been widely studied for RNA [273], but such examples are limited for XNAs other than DNA and RNA. However, systems that have been studied in this context include pRNA [274, 275] and the acyclic threonine derivative L-aTNA [276], which allow for pRNA ligation on pRNA templates and L-aTNA ligation on L-aTNA templates, respectively.

Further, in the context of ligation, it is noteworthy that some XNAs such as HNA, TNA, and LNAs can be accessed by enzymatic ligation reactions [266, 277–279]. Moreover, other chemoenzymatic methods are currently being developed for the synthesis of XNA oligonucleotides [280–282].

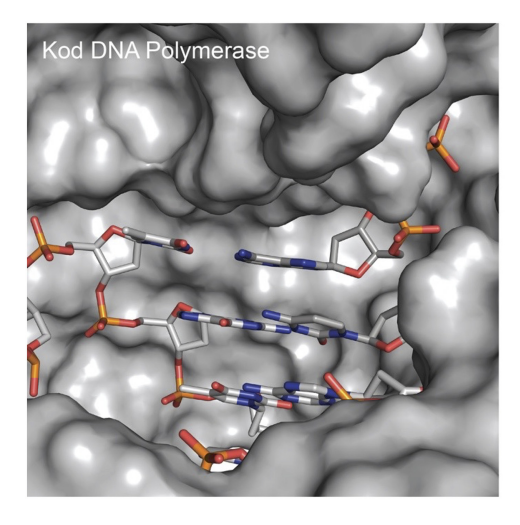
RNA-dependent RNA Pol ribozymes evolved *in vitro* offer valuable tools for studying XNA synthesis in the absence of protein enzymes. One interesting example is an RNA-dependent RNA Pol ribozyme that exhibits varying levels of promiscuity toward XNAs, both as monomers and as templates [283], implying that ribozymes could have enabled evolutionary transitions between different types of early genetic systems. A second important example is a cross-chiral RNA

Pol ribozyme capable of copying RNA of the opposite chiral handedness, such that L-RNA information is copied into D-RNA and vice versa [284]. This class of ribozymes overcomes the well-characterized problem of cross-chiral inhibition in which nonenzymatic polymerization reactions of D-RNA were inhibited by the presence of L-RNA monomers [285].

Aptamers—nucleic acid molecules that mimic antibodies by folding into structures with ligand binding sites that are complementary in size and shape to specific targets—hold significant potential as future diagnostic and therapeutic agents [286–288]. Although some aptamers exist naturally as the ligand binding domain of riboswitches [289], most are identified by in vitro selection approaches that mimic Darwinian evolution [290]. While structural insights into the ligand binding properties of DNA and RNA aptamers are well established [291], often relying on induced fit to optimize intramolecular interactions for cognate target binding, very little is known about the ability for XNA aptamers to fold and function. Modeling of an HNA aptamer bound to hen eggwhite lysozyme features a hGhT-rich motif with non-Watson-Crick interactions [292], suggesting a diverse repertoire of structural conformations may be available to XNA aptamers. Advances in the development of base-modified TNA aptamers have established parallelizable paths for generating high affinity sequences from single-round screening approaches mirroring those of DNA-encoded small molecule libraries [293]. The ability to query diverse library chemotypes while avoiding the need for iterative rounds of selection offers a promising strategy for accelerating the discovery of therapeutic aptamers.

Natural Pols including those from thermophilic organisms [294, 295] and trans-lesion and repair Pols [296] are in some cases able to handle certain XNAs, albeit often with reduced efficiency of catalysis. Early work in this area showed that certain DNA polymerases could synthesize short segments of DNA on TNA templates [297], while other polymerases could synthesize limited amounts of TNA on DNA templates [298– 301]. Similar results were also observed for FANA and HNA replication systems [302–305]. Bst DNA pol (A-family), an analog of E. coli DNA polymerase I, stands out as an interesting natural polymerase due to its ability to reverse transcribe diverse XNA templates into DNA [306]. Indeed, this enzyme is still used today to reverse transcribe TNA into DNA [306]. These early studies laid the foundation for subsequent polymerase engineering efforts that made it possible to replicate XNAs in the laboratory by copying genetic information back and forth between DNA and XNA. For an exhaustive review on Pol engineering see reference [307].

The development of engineered XNA Pols led to the isolation of TNA and HNA aptamers with specific protein-binding activity from large combinatorial libraries [308, 309]. Although an important landmark in the newly minted field of synthetic genetics [11, 310], the modest activity of first-generation XNA Pols limited their use in downstream applications [9]. XNA Pol reactions performed at that time required long extension times and the presence of manganese ions in the reaction mixture to reduce the substrate specificity of the enzyme against XNA, either in the template or as triphosphates [297, 298, 305]. Fortunately, continued advances in the development of Pol engineering technologies, including the use of ultra-high throughput microfluidic screening platforms, like droplet-based optical Pol sorting [311], have enabled the



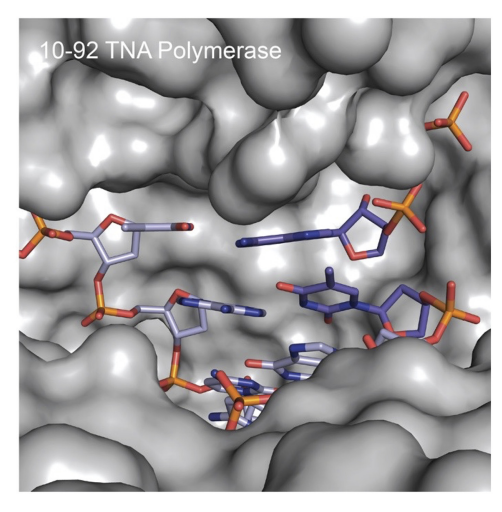


Figure 11. Active site view of natural Kod DNA Pol and the engineered 10-92 TNA Pol.

discovery of XNA Pols with activities approaching their natural counterparts. One exciting example in this area is a TNA Pol called 10–92 (Fig. 11) that can achieve a catalytic rate of  $\sim 1$  nts $^{-1}$  and > 99% fidelity [312]. An X-ray crystal structure of the catalytically active conformation reveals large conformational changes relative to its closest natural homolog, indicating that the evolutionary distance required to transition natural DNA Pols into highly specialized XNA Pols may be greater than previously thought [312]. As work in this area continues, it will be interesting to see how closely Pols engineering efforts can mimic the activity of natural enzymes, and the degree of structural change required to achieve such levels of activity.

### XNA therapeutics

From 1998 to 2025, the United States Food and Drug Administration (FDA) approved 25 oligonucleotide therapeutics. These include seven antisense oligonucleotides, five spliceswitching oligonucleotides, two aptamers, six small interfering RNAs (siRNAs), two vaccine adjuvants, two mRNA COVID-19 vaccines, and one telomerase inhibitor [214]. Common chemical modifications found in these drugs include substitution of the 2' hydroxyl position of ribose with fluorine (2'F RNA), methoxy (2'-OMe RNA), 2'-O-(2-methoxyethyl) (MOE RNA) groups, phosphorothioate linkages (PS), and nucleobase substitutions, such 5-methyl cytosine and N1-methyl pseudouridine (mRNA vaccines). Another XNA modification found in oligonucleotide therapeutics currently in clinical use is the phosphorodiamidate morpholino (PMO) analog. It is used exclusively in splice-switching oligonucleotides (SSOs) targeting different exons of dystrophin mRNA for the treatment of Duchenne muscular dystrophy (DMD), specifically in the drugs Exondys 51, Vyondys 53, Viltepso, and Amondys 45 [313, 314].

In some applications, achieving a strong pairing between nucleotides may not always be desirable. For example, a comparison of *in vivo* RNAi silencing potencies targeting factor VII between siRNAs containing 2'-F RNA, 2'-OMe RNA, MOE-RNA, and LNA pyrimidines showed that 2'-F RNA was the most effective analog [315], illustrating the idiosyncrasies of drug discovery. Interestingly, while the 2'-F modification is

highly effective, it provides less of a boost to thermal stability compared to the MOE-RNA and LNA analogs [315]. Thermal rebalancing in critical regions of siRNA duplexes and the strategic introduction of destabilizing modifications are key concepts in the design of RNAi therapeutics. These strategies have led to breakthroughs, such as the use of chiral acyclic (*S*)-GNA, which have helped mitigate off-target effects [214].

Further insights can be gained from crystal structures of human Argonaute 2 (Ago2) in complex with miRNA single strands or siRNA duplexes. These structures reveal a strong kink in the antisense siRNA near the 3'-end of the seed region, between residues AS6 and AS7 [316, 317]. The distance between adjacent phosphorus atoms in the antisense siRNA at the kink is as short as 5.5 Å. Three Ago2 side chains—Ile-365, Gln-757, and Ile-756—straddle the minor groove of the seed region. The glutamine side chain forms a H-bond with the 2' hydroxyl group of AS6 (Fig. 12). The electrostatic repulsion caused by closely spaced phosphates at the kink is offset by a cluster of three arginine residues, along with lysine and histidine, which gather around the AS6 to AS8 phosphate moieties.

The kink in the RNA structure results in tighter spacing between adjacent phosphates, a feature that can be mimicked by (S)-GNA and TNA (Table 1, Fig. 13). Both XNAs have only five bonds between phosphates in their backbones, compared to six in standard DNA and RNA. This naturally matches the 5.5 Å spacing observed between phosphates in kinked antisense siRNA bound to Ago2. (S)-GNA and TNA can cross-pair with RNA but incorporating single nucleotides or base pairs into RNA results in significant destabilization of pairing.

When these XNAs were walked along both antisense and sense strand siRNAs, *in vitro* activity measurements showed that both (*S*)-GNA and TNA were tolerated at several sites [316, 319]. In particular, substitutions at positions AS6 and AS7 (Fig. 12) led to increased potency. This effect is thought to stem from local softening of pairing constraints and preorganization of the antisense siRNA to favor the kinked conformation. AltNA, which also features closer spacing between adjacent phosphates (Fig. 13), was similarly tested. When AltNA residues were placed at the kink site, beneficial effects on activity were observed [320]. The importance of preorganizing the antisense siRNA for the kinked conformation in enhancing activity was further confirmed by the favorable ac-

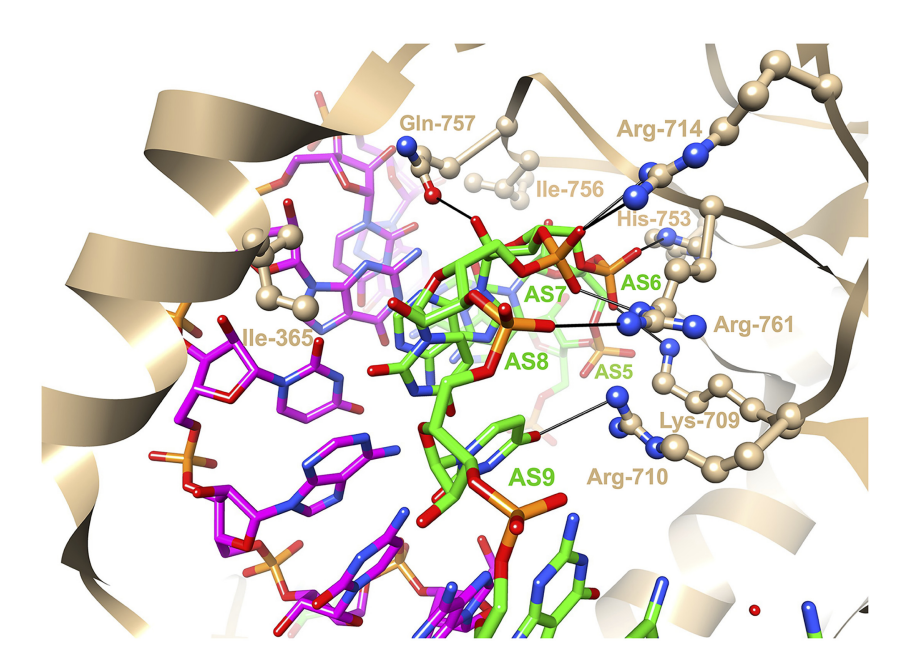


Figure 12. View across the minor groove of the siRNA antisense-/sense-strand duplex bound to Ago2 [318]; PDB ID 4w5t). Carbon atoms of the antisense and sense strands are colored in green and magenta, respectively. Selected Ago2 side chains and antisense siRNA residues are labeled, and H-bonds and salt bridges are indicated with thin solid lines.

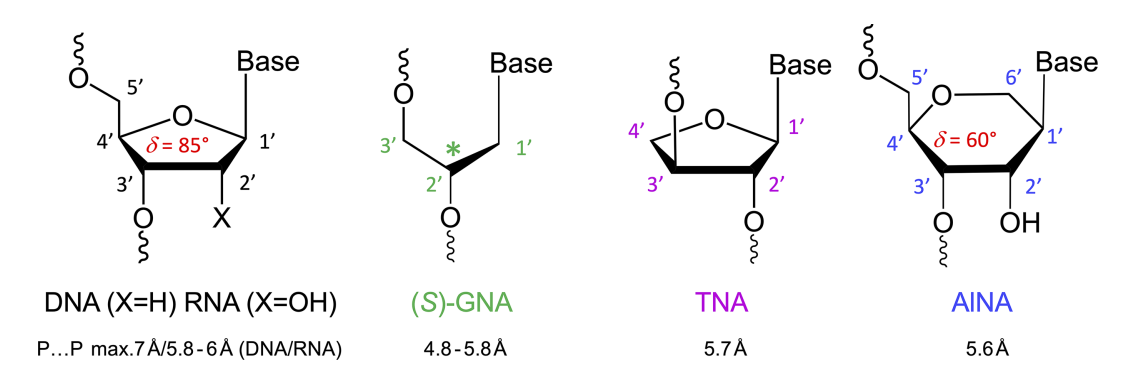


Figure 13. Structures of DNA, RNA, (S)-GNA, TNA, and AltNA. Distances below the structures correspond to average spacings between phosphorus atoms of 5'- and 3'-phosphates (B-DNA, A-RNA, and AltNA) and 3'- and 2'-phosphates (GNA, TNA).

tivity of siRNA incorporating 2'-deoxy-2'- $\alpha$ -F-2'- $\beta$ -C-methyl (gem-2'-F/Me) nucleotides at positions AS6 or AS7 [321]. While this modification does not reduce phosphate spacing, computational models suggest that the methyl group of gem-2'-F/Me pushes away the neighboring nucleobase, triggering a roll-bend that resembles the kinked conformation seen with native RNA.

Besides the beneficial effects for potency and safety of therapeutic siRNA candidates containing the abovementioned XNA residues, it is worth mentioning that placement of a 2'-5' RNA modification at AS7 was shown to significantly reduce siRNA seed-mediated binding to off-target transcripts while maintaining on-target activity [172]. Earlier investigations directed at the effects of 2'-5' linkages inside siRNA on RNAi activity had established that such modifications were generally well tolerated inside the sense strand but only at a few positions in the antisense strand [322]. Thus, 5'-phosphorylation of the siRNA antisense strand was minimally affected by the presence of a 2'-5' linkage between AS1 and AS2. However, several modifications inside the antisense strand negatively affected siRNA loading into Ago2. Of note is the finding that 2'-

5' linkages abrogated the immune-stimulatory effects of modified siRNAs.

Clinically, the beneficial effects of XNAs at certain positions of antisense siRNA observed in vitro translated into increased potencies in vivo. Notably, the inclusion of (S)-GNA and TNA at position AS7 mitigated off-target effects. Although these two XNAs share similarities, they do not pair with one another [323]. A unique feature of the (S)-GNA duplex is its adoption of a right-handed A-form-like backbone conformation, combined with an inverted base pair orientation within the stack [214, 215]. GNA does not align with RNA when incorporated into the siRNA duplex, retaining its flipped nucleobase orientation opposite the RNA pairing partner. The destabilization of G:C pairs, relative to A:U pairs, can be offset by substituting iso-C or iso-G GNA residues opposite ribo-G or ribo-C, respectively [102]. The GalNAc-conjugate enhanced stability chemistry (ESC+), which incorporates (S)-GNA at position AS7 for liver delivery, has significantly improved potency and clinical safety due to seed pairing destabilization and conformational preorganization [172]. Importantly, this effect cannot be replicated by simply incorporating 2'-deoxyribonucleotides into the seed region to modulate thermal stability.

Two siRNAs in clinical development—ALN-AAT, that targets the Alpha-1 antitrypsin gene, and ALN-HBV, that targets Hepatitis B virus—were initially found to cause transient, asymptomatic liver enzyme elevations in a dose-dependent manner in patients [214, 215]. Similar elevations had been observed in preclinical rodent studies, but the hepatotoxicity was attributed to specific sequences rather than modification chemistry. The ESC+ approach, which mitigates off-target effects and improves safety, prompted the redesign of ALN-AAT and ALN-HBV by incorporating a single (S)-GNA residue at the AS7 seed region (ALN-AAT02 and ALN-HBV02, respectively) [214]. These modified siRNAs were evaluated in a Phase I study with healthy volunteers, demonstrating improved preclinical safety profiles. Neither siRNA led to elevated liver enzyme levels at the highest dose, confirming the benefits of the ESC+ design approach and the advantage of incorporating XNA at specific sites.

Several ESC+ candidate siRNAs with GNA incorporation are currently in clinical development, with ALN-HBV02 having advanced to Phase II trials. Currently, GNA has only been applied to RNAi therapeutics. However, we expect that more candidate therapeutics using various modalities that target a plethora of human diseases [324–327] and modified with XNAs beyond those in already approved drugs will enter the clinic in the coming years.

### **Conclusions**

XNAs, defined as sugar-modified nucleic acids, were first introduced in the context of synthetic biology. Their nomenclature spans the entire alphabet of 26 letters with their sugar moiety defining their position in the alphabet. XNAs can be categorized into those that hybridize with natural nucleic acids and those that do not. Structural parameters such as sugar puckering, inclination angle, and helical twist may help further classify them into subgroups of related systems.

XNAs that cross-pair with DNA and RNA have been extensively studied for their potential in therapeutic and diagnostic applications, particularly in interactions with cellular biology [328]. This field has greatly advanced with the clinical use of antisense, splice-switching, siRNA and aptamer drugs featuring chemically modified RNA mimics like 2′-OMe, 2′-F, 2′-MOE, and PMO which have been retrospectively classified as XNAs. Among these, TNA, HNA, and PNA hold a unique position, as they were the first XNAs designed without using DNA or RNA chemistry as a blueprint, yet they hybridize with natural nucleic acids. Their discovery was influenced by considerations of the origin of life and the structural folding of other bioorganic molecules, such as carbohydrates and peptides.

Representative orthogonal XNAs include pRNA, XyloNA, and L-DNA, whereby the latter has been utilized as a genetic system for aptamer development. The field of XNA research remains in its early stages and presents additional complexity, as it requires selecting XNAs that function as agonists *in vivo* rather than antagonists. A promising development is the discovery of key tools such as XNA Pols and ligases, although we are still far from an orthogonal replication system capable of evolving and encoding new functions within a cell. However, it is noteworthy that faithful transcription using a chemically

synthesized, mirror-image T7 RNA Pol of L-RNA 5S, 16S, and 23S rRNAs has been achieved from L-DNA genes [329].

While therapeutics and diagnostics constitute important fields for XNA applications, these nucleic acid analogs are also used in other practical applications. For examples in bio- and nanotechnology, see e.g. CeNA, FANA, and HNA nanostructures visualized by TEM [330], FANA nanostructures as stable carriers for cellular delivery [331], TNA-shielded DNA nanostructures [332], and HNA as glue triggering the controlled formation of bacterial tissues [333]. In the realm of drug discovery, complementary PNA oligonucleotides mediated assembly of a supramolecular inhibitor of thrombin whose action was reversed with an antidote oligo [334].

### Acknowledgements

We would like to thank A. Ngor, Y. Jia, and Q. Li their assistance with the XNA table, and members of the Chaput, Egli, and Herdewijn labs for helpful discussions.

Author contributions: J.C.C., M.E., and P.H. contributed equally to this article.

### **Conflict of interest**

The authors do not report any conflicts of interest.

### **Funding**

This work was supported by NIH grants R01 ES029357 and P01 CA160032 (M.E.), NSF grant 2 224 897 (MCB to M.E.), Vanderbilt University, and NSF grant 2 433 788 (CLP/GM to J.C.). Funding to pay the Open Access publication charges for this article was provided by Invited CR&P articles are published open access at no cost to the authors. M.E. is a member of the NAR editorial board.

### Data availability

Table 1 is limited to XNA systems that have been incorporated into oligonucleotides and is currently maintained at https://chaputlab.com/xna-alphabet/.

#### References

- Watson JD, Crick FH. Molecular structure of nucleic acids; a structure for deoxyribose nucleic acid. *Nature* 1953;171:737–8. https://doi.org/10.1038/171737a0
- Dickerson R, Bansal M, Calladine C et al. Definitions and nomenclature of nucleic acid structure parameters. EMBO J 1989;8:1–4.
- Lu XJ, Olson WK. 3DNA: a versatile, integrated software system for the analysis, rebuilding and visualization of three-dimensional nucleic-acid structures. *Nat Protoc* 2008;3:1213–27. https://doi.org/10.1038/nprot.2008.104
- 4. Pallan PS, Lubini P, Bolli M *et al.* Backbone-base inclination as a fundamental determinant of nucleic acid self- and cross-pairing. *Nucleic Acids Res* 2007;35:6611–24. https://doi.org/10.1093/nar/gkm612
- Vicens Q, Kieft JS. Thoughts on how to think (and talk) about RNA structure. Proc Natl Acad Sci USA 2022;119:e2112677119. https://doi.org/10.1073/pnas.2112677119
- Watson JD, Crick FH. Genetical implications of the structure of deoxyribonucleic acid. *Nature* 1953;171:964–7. https://doi.org/10.1038/171964b0

- Chaput JC, Herdewijn P. What is XNA? Angew Chem Int Ed 2019;58:11570–2. https://doi.org/10.1002/anie.201905999
- Anosova I, Kowal EA, Dunn MR et al. The structural diversity of artificial genetic polymers. Nucleic Acids Res 2016;44:1007–21. https://doi.org/10.1093/nar/gkv1472
- Chaput JC. Redesigning the genetic polymers of life. Acc Chem Res 2021;54:1056–65. https://doi.org/10.1021/acs.accounts.0c00886
- 10. Joyce GF. Toward an alternative biology. Science 2012;336:307–8. https://doi.org/10.1126/science.1221724
- Chaput JC, Yu H, Zhang S. The emerging world of synthetic genetics. *Chem Biol* 2012;19:1360–71. https://doi.org/10.1016/j.chembiol.2012.10.011
- Pinheiro VB, Loakes D, Holliger P. Synthetic polymers and their potential as genetic materials. *Bioessays* 2013;35:113–22. https://doi.org/10.1002/bies.201200135
- 13. Kim SC, Zhou L, Zhang W *et al.* A model for the emergence of RNA from a prebiotically plausible mixture of ribonucleotides, arabinonucleotides, and 2'-deoxynucleotides. *J Am Chem Soc* 2020;5:2317–26. https://doi.org/10.1021/jacs.9b11239
- 14. Eschenmoser A. Chemical etiology of nucleic acid structure. *Science* 1999;284:2118–24. https://doi.org/10.1126/science.284.5423.2118
- Egli M, Lubini P, Pallan PS. The long and winding road to the structure of homo-DNA. *Chem Soc Rev* 2007;36:31–45. https://doi.org/10.1039/B606807C
- Gilbert W. The RNA world. Nature 1986;319:618. https://doi.org/10.1038/319618a0
- 17. Taylor AI, Houlihan G, Holliger P. Beyond DNA and RNA: the expanding toolbox of synthetic genetics. *Cold Spring Harb Perspect Biol* 2019;11, a032490. https://doi.org/10.1101/cshperspect.a032490
- 18 . Bian T, Pei Y, Gao S et al. Xeno nucleic acids as functional materials: from biophysical properties to application. Adv Healthc Mater 2024;13:e2401207. https://doi.org/10.1002/adhm.202401207
- Morihiro K, Kasahara Y, Obika S. Biological applications of xeno nucleic acids. *Mol BioSyst* 2017;13:235–45.https://doi.org/10.1039/C6MB00538A
- Koshkin AA, Nielsen P, Meldgaard M et al. LNA (locked nucleic acid): an RNA mimic forming exceedingly stable LNA:LNA duplexes. J Am Chem Soc 1998;120:13252–3. https://doi.org/10.1021/ja9822862
- Martin P. A new access to 2'-O-alkylated ribonucleosides and properties of 2'-O-alkylated oligoribonucleotides. *Helv Chim Acta* 1995;78:486–504. https://doi.org/10.1002/hlca.19950780219
- 22. Teplova M, Minasov G, Tereshko V *et al.* Crystal structure and improved antisense properties of 2'-O-(2-methoxyethyl)-RNA. *Nat Struct Biol* 1999;6:535–9.
- 23. Wilds CJ, Damha MJ.
  2'-Deoxy-2'-fluoro-beta-D-arabinonucleosides and oligonucleotides (2'F-ANA): synthesis and physicochemical studies. *Nucleic Acids Res* 2000;28:3625–35. https://doi.org/10.1093/nar/28.18.3625
- 24. Berger I, Tereshko V, Ikeda H et al. Crystal structures of B-DNA with incorporated 2'-deoxy-2'-fluoro-arabino-furanosyl thymines: implications of conformational preorganization for duplex stability. Nucleic Acids Res 1998;26:2473–80. https://doi.org/10.1093/nar/26.10.2473
- 25. Nielsen PE, Egholm M, Berg RH *et al.* Sequence-selective recognition of DNA by strand displacement with a thymine-substituted polyamide. *Science* 1991;254:1497–500. https://doi.org/10.1126/science.1962210
- 26. Saarbach J, Sabale PM, Winssinger N. Peptide nucleic acid (PNA) and its applications in chemical biology, diagnostics, and therapeutics. *Curr Opin Chem Biol* 2019;52:112–24.
- 27. Gessler K, Uson I, Takaha T *et al.* V-amylose at atomic resolution: x-ray structure of a cycloamylose with 26 glucose

- residues (cyclomaltohexaicosaose). *Proc Natl Acad Sci USA* 1999;**96**:4246–51. https://doi.org/10.1073/pnas.96.8.4246
- 28 . Herdewijn P. Nucleic acids with a six-membered 'carbohydrate' mimic in the backbone. *Chem Biodivers* 2010;7:1–59. https://doi.org/10.1002/cbdv.200900185
- 29. Schoning K, Scholz P, Guntha S et al. Chemical etiology of nucleic acid structure: the alpha-threofuranosyl-(3'→2') oligonucleotide system. Science 2000;290:1347–51. https://doi.org/10.1126/science.290.5495.1347
- Pitsch S, Wendeborn S, Jaun B et al. Why pentose and not hexose nucleic acids? Part VII. Pyranosyl-RNA ('p-RNA'). Helv Chim Acta 1993;76:2161–83. https://doi.org/10.1002/hlca.19930760602
- 31. Maiti M, Maiti M, Knies C *et al.* Xylonucleic acid: synthesis, structure, and orthogonal pairing properties. *Nucleic Acids Res* 2015;43:7189–200. https://doi.org/10.1093/nar/gkv719
- 32. Klussmann S, Nolte A, Bald R *et al.* Mirror-image RNA that binds D-adenosine. *Nat Biotechnol* 1996;14:1112–5. https://doi.org/10.1038/nbt0996-1112
- Adamala KP, Agashe D, Belkaid Y et al. Confronting risks of mirror life. Science 2024;386:1351–3. https://doi.org/10.1126/science.ads9158
- 34 . Ribas de Pouplana Ls. The Genetic Code and the Origin of Life. New York, N.Y.: Landes Bioscience/Eurekah.com; Kluwer Academic/Plenum, Georgetown, Tex, 2004
- Thibaudeau C, Acharya P, Chattopadhyaya J. Stereoelectronic Effects in Nucleosides and Nucleotides and Their Structural Implications. Uppsala, Sweden: Uppsala University Press, 2005
- Blackburn GM, Egli M, Gait MJ et al. Nucleic Acids in Chemistry and Biology. 4th edition. London, UK: Royal Society of Chemistry, 2022
- 37. Pearl LH. Structure and function in the uracil-DNA glycosylase superfamily. *Mutat Res* 2000;460:165–81. https://doi.org/10.1016/S0921-8777(00)00025-2
- Lesk AM. Why does DNA contain thymine and RNA uracil? *J Theor Biol* 1969;22:537–40. https://doi.org/10.1016/0022-5193(69)90021-6
- 39. Marathe A, Bansal M. The 5-methyl group in thymine dynamically influences the structure of A-tracts in DNA at the local and global level. *J Phys Chem B* 2010;114:5534–46. https://doi.org/10.1021/jp911055x
- 40. Plavec J, Thibaudeau C, Chattopadhyaya J. How does the 2'-hydroxy group drive the pseudorotational equilibrium in nucleoside and nucleotide by the tuning of the 3'-gauche effect? *J Am Chem Soc* 1994;116:6558–60. https://doi.org/10.1021/ja00094a009
- 41. Pallan PS, Wilds CJ, Wawrzak Z *et al.* Why does TNA cross-pair more strongly with RNA than with DNA? An answer from X-ray analysis. *Angew Chem Int Ed* 2003;42:5893–5. https://doi.org/10.1002/anie.200352553
- 42. Wilds CJ, Wawrzak Z, Krishnamurthy R et al. Crystal structure of a B-form DNA duplex containing-alpha-threofuranosyl (3'→2') nucleosides: a four-carbon sugar is easily accommodated into the backbone of DNA. J Am Chem Soc 2002;124:13716–21. https://doi.org/10.1021/ja0207807
- 43. Ebert M-O, Mang C, Krishnamurthy R et al. The structure of a TNA-TNA complex in solution: NMR study of the octamer duplex derived from a-(L)-threofuranosyl-(3'-2')-CGAATTCG. J Am Chem Soc 2008;130:15105–15. https://doi.org/10.1021/ja8041959
- 44. Freier SM, Altmann K-H. The ups and downs of nucleic acid duplex stability: structure-stability studies on chemically modified DNA:RNA duplexes. *Nucleic Acids Res* 1997;25:4429–43. https://doi.org/10.1093/nar/25.22.4429
- 45. Lind KE, Mohan V, Manoharan M *et al.* Structural characteristics of 2'-O-(2-methoxyethyl)-modified nucleic acids from molecular dynamics simulations. *Nucleic Acids Res* 1998;26:3694–9. https://doi.org/10.1093/nar/26.16.3694

- 46. Gryaznov SM, Lloyd DH, Chen JK et al. Oligonucleotide N3'→P5' phosphoramidates. Proc Natl Acad Sci USA 1995;92:5798–802. https://doi.org/10.1073/pnas.92.13.5798
- 47. Tereshko V, Gryaznov SM, Egli M. Consequences of replacing the DNA 3'-oxygen by an amino group: high-resolution crystal structure of a fully modified N3'→P5' phosphoramidate DNA dodecamer duplex. *J Am Chem Soc* 1998;120:269–83. https://doi.org/10.1021/ja971962h
- 48. Rigl CT, Lloyd DH, Tsou DS *et al.* Structural RNA mimetics: N3'→P5' phosphoramidate DNA analogs of HIV-1 RRE and TAR RNA form A-type helices that bind specifically to rev and Tat-related peptides. *Biochemistry* 1997;36:650–9. https://doi.org/10.1021/bi961980w
- 49. Acharya P, Acharya S, Cheruku P et al. Cross-modulation of the pKa of nucleobases in a single-stranded hexameric-RNA due to tandem electrostatic nearest-neighbor interactions. J Am Chem Soc 2003;125:9948–61. https://doi.org/10.1021/ja034651h
- 50. Thibaudeau C, Plavec J, Chattopadhyaya J. Quantitation of the pD dependent thermodynamics of the N 

  S pseudorotational equilibrium of the pentofuranose moiety in nucleosides gives a direct measurement of the strength of the tunable anomeric effect and the pKa of the nucleobase. *J Org Chem* 1996;61:266–86. https://doi.org/10.1021/jo951124a
- 51. Velikian I, Acharya P, Trifonova A *et al.* The RNA molecular wire: the pH-dependent change of the electronic character of adenin-9-yl is transmitted to drive the sugar and phosphate torsions in adenosine 3',5'-bisphosphate. *J Phys Org Chem* 2000;13:300–5. https://doi.org/10.1002/1099-1395(200005)13: 5%3c300::AID-POC245%3e3.0.CO;2-W
- 52. Acharya P, Trifonova A, Thibaudeau C et al. The transmission of the electronic character of guanin-9-yl drives the sugar-phosphate backbone torsions in guanosine 3',5'-bisphosphate. Angew Chem Int Ed 1999;38:3645–50. https://doi.org/10.1002/(SICI)1521-3773(19991216)38: 24%3c3645::AID-ANIE3645%3e3.0.CO;2-O
- 53. Giannaris PA, Damha MJ. Oligoribonucleotides containing 2',5'-phosphodiester linkages exhibit binding selectivity for 3',5'-RNA over 3',5'-ssDNA. *Nucl Acids Res* 1993;21:4742–9. https://doi.org/10.1093/nar/21.20.4742
- 54. Engelhart AE, Powner MW, Szostak JW. Functional RNAs exhibit tolerance for non-heritable 2'-5' versus 3'-5' backbone heterogeneity. *Nature Chem* 2013;5:390–4. https://doi.org/10.1038/nchem.1623
- 55. Li L, Szostak JW. The free energy landscape of pseudorotation in 3'-5' and 2'-5' linked nucleic acids. J Am Chem Soc 2014;136:2858–65. https://doi.org/10.1021/ja412079b
- Shen F, Luo Z, Liu H et al. Structural insights into RNA duplexes with multiple 2'-5'-linkages. Nucleic Acids Res 2017;45:3537-46.
- Mutschler H, Taylor AI, Porebski BT *et al.* Random-sequence genetic oligomer pools display an innate potential for ligation and recombination. *eLife* 2018;7:e43022. https://doi.org/10.7554/eLife.43022
- 58 . Maiti M, Siegmund V, Abramov M et al. Solution structure and conformational dynamics of deoxyxylonucleic acids (dXNA): an orthogonal nucleic acid candidate. Chem A Eur J 2012;18:869–79. https://doi.org/10.1002/chem.201102509
- Leontis NB, Lescoute A, Westhof E. The building blocks and motifs of RNA architecture. Curr Opin Struct Biol 2006;16:279–87. https://doi.org/10.1016/j.sbi.2006.05.009
- 60. Cappannini A, Ray A, Purta E et al. MODOMICS: a database of RNA modifications and related information. 2023 update. Nucleic Acids Res 2024;52:D239–44. https://doi.org/10.1093/nar/gkad1083
- Hombach S, Kretz M. Non-coding RNAs: classification, biology and functioning. Adv Exp Med Biol 2016;937:3–17. https://link.springer.com/chapter/10.1007/978-3-319-42059-2\_1
- 62. Yelland JN, Bravo JPK, Black JJ et al. A single 2'-O-methylation of ribosomal RNA gates assembly of a functional ribosome. Nat

- *Struct Mol Biol* 2023;**30**:91–8. https://doi.org/10.1038/s41594-022-00891-8
- 63. Ng EWM, Shima DT, Calias P et al. Pegaptanib, a targeted anti-VEGF aptamer for ocular vascular disease. Nat Rev Drug Discov 2006;5:123–32. https://doi.org/10.1038/nrd1955
- Mullard A. FDA approves second RNA aptamer. *Nat Rev Drug Discov* 2023;22:774. https://doi.org/10.1038/d41573-023-00148-z
- 65. Luo M, Groaz E, Froeyen M et al. Invading Escherichia coli genetics with a xenobiotic nucleic acid carrying an acyclic phosphonate backbone (ZNA). J Am Chem Soc 2019;141:10844–51. https://doi.org/10.1021/jacs.9b04714
- 66. Petrova M, Pav O, Budesinsky M *et al.* Straightforward synthesis of purine 4'-alkoxy-2'-deoxynucleosides: first report of mixed purine-pyrimidine 4'-alkoxyoligodeoxynucleotides as new RNA mimics. *Org Lett* 2015;17:3426–9. https://doi.org/10.1021/acs.orglett.5b01430
- 67. Cicero D, Gallo M, Neuner P *et al.* Synthesis and properties of (2'S)- and (2'R)-2'-deoxy-2'-C-methyl olgonucleotides. *Tetrahedron* 2001;57:7613–21. https://doi.org/10.1016/S0040-4020(01)00745-1
- 68. Wang G, Middleton P, Lin C *et al.* Biophysical and biochemical properties of oligodeoxynucleotides containing 4'-C and 5'-C substituted thymidines. *Bioorg Med Chem Lett* 1999;9:885–90. https://doi.org/10.1016/S0960-894X(99)00103-1
- 69. Saha A, Caulfield T, Hobbs C et al. 5'-Me-DNA-A new oligonucleotide analog: synthesis and biochemical properties. J Org Chem 1995;60:788–9. https://doi.org/10.1021/jo00109a003
- Damha MJ, Usman N, Ogilvie KK. Solution and solid-phase chemical synthesis of arabinonucleotides. *Can J Chem* 1989;67:831–9. https://doi.org/10.1139/v89-129
- Allart B, Khan K, Rosemeyer H et al. D-altritol nucleic acids (ANA): hybridisation properties, stability, and initial structural analysis. Chem Eur J 1999;5:2424–31. https://chemistry-europe.onlinelibrary.wiley.com/doi/10.1002/ (SICI)1521-3765(19990802)5:8%3C2424:: AID-CHEM2424%3E3.0.CO;2-W
- 72. Egli M, Pallan PS, Allerson CR et al. Synthesis, improved antisense activity and structural rationale for the divergent RNA affinities of 3'-fluoro hexitol nucleic acid (FHNA and Ara-FHNA) modified oligonucleotides. J Am Chem Soc 2011;133:16642–9. https://doi.org/10.1021/ja207086x
- Zhou D, Lagoja IM, Rozenski J et al. Synthesis and properties of aminopropyl nucleic acids. ChemBioChem 2005;6:2298–304. https://doi.org/10.1002/cbic.200500170
- 74. Hendrix C, Devreese B, Rozenski J et al. Incorporation of 2'-amido-nucleosides in oligodeoxynucleotides and oligoribonucleotides as a model for 2'-linked conjugates. Nucl Acids Res 1995;23:51–7. https://doi.org/10.1093/nar/23.1.51
- 75. Kataoka M, Kouda Y, Sato K *et al.* Highly efficient enzymatic synthesis of 3'-deoxyapionucleic acid (apioNA) having the four natural nucleobases. *Chem Commun* 2011;47:8700–2. https://doi.org/10.1039/c1cc12980e
- 76. Hobbs J, S Sternbac.H, M et al. Polynucleotides containing 2'-amino-2'-deoxyribose and 2'-azido-2'-deoxyribose. Biochemistry 1973;12:5138–45. https://doi.org/10.1021/bi00749a018
- 77. Yahara A, Shrestha AR, Yamamoto T et al. Amido-bridged nucleic acids (AmNAs): synthesis, duplex stability, nuclease resistance, and in Vitro antisense potency. ChemBioChem 2012;13:2513–6. https://doi.org/10.1002/cbic.201200506
- 78. Tarkoy M, Bolli M, Leumann C. Nucleic-acid analogs with restricted conformational flexibility in the sugar-phosphate backbone (Bicyclo-DNA) .3. Synthesis, pairing properties, and calorimetric determination of duplex and triplex stability of decanucleotides from [(3's,5'r)-2'-Deoxy-3',5'-Ethano-Beta-D-Ribofuranosyl]adenine and thymine. Helv Chim Acta 1994;77:716–44.

- Epple C, Leumann C. Bicyclo[3.2.1]-DNA, a new DNA analog with a rigid backbone and flexibly linked bases: pairing properties with complementary DNA. *Chem Biol* 1998;5:209–16.
- Ahn DR, Egger A, Lehmann C et al. Bicyclo[3.2.1]amide-DNA: a chiral, nonchiroselective base-pairing system. Chem Eur J 2002;8:5312–22. https://chemistry-europe.onlinelibrary.wiley.com/doi/10.1002/1521-3765(20021202)8:23%3C5312:: AID-CHEM5312%3E3.0.CO;2-M
- Stauffiger A, Leumann CJ. Screening the structural space of bicyclo-DNA: synthesis and thermal melting properties of bc-DNA. Eur J Org Chem 2009;2009:1153–62. https://doi.org/10.1002/ejoc.200801034
- 82. Nielsen P, Pfundheller HM, Olsen CE *et al.* Synthesis of 2'-O,3'-C-linked bicyclic nucleosides and bicyclic oligonucleotides. *J Chem Soc*, *Perkin Trans* 1 1997;1:3423–34. https://doi.org/10.1039/a703176i
- Kumar V, Gore KR, Pradeepkumar PI et al. Design, synthesis, biophysical and primer extension studies of novel acyclic butyl nucleic acid (BuNA). Org Biomol Chem 2013;11:5853–65.
- 84. Sagi J, Szemzo A, Szecsi J *et al.* Biochemical properties of oligo [(+)-carbocyclic-thymidylates] and their complexes. *Nucl Acids Res* 1990;18:2133–40. https://doi.org/10.1093/nar/18.8.2133
- 85. Maurinsh Y, Rosemeyer H, Esnouf R et al. Synthesis and pairing properties of oligonucleotides containing 3-hydroxy-4-hydroxymethyl-1-cyclohexanyl nucleosides. Chem Eur J 1999;5:2139–50. https://chemistry-europe.onlinelibrary.wiley.com/doi/10.1002/(SICI)1521-3765(19990702)5: 7%3C2139::AID-CHEM2139%3E3.0.CO;2-K
- 86. Paolella C, D'Alonzo D, Schepers G et al. Oligonucleotides containing a ribo-configured cyclohexanyl nucleoside: probing the role of sugar conformation in base pairing selectivity. Org Biomol Chem 2015;13:10041–9.
- 87. Wang J, Verbeure B, Luyten I *et al.* Cyclohexene nucleic acids (CeNA): serum stable oligonucleotides that activate RNase H and increase duplex stability with complementary RNA. *J Am Chem Soc* 2000;122:8595–602. https://pubs.acs.org/doi/10.1021/ja000018%2B
- 88. Gu P, Morral J, Wang J *et al.* Synthesis and biological evaluation of a series of new cyclohexenyl nucleosides. *Nucleosides Nucleotides Nucleic Acids* 2003;22:845–7. https://doi.org/10.1081/NCN-120022668
- Stirchak EP, Summerton JE, Weller DD. Uncharged stereoregular nucleic-acid analogs .1. Synthesis of a cytosine-containing oligomer with carbamate internucleoside linkages. J Org Chem 1987;52:4202–6. https://doi.org/10.1021/jo00228a010
- Ni G, Du Y, Tang F et al. Review of alpha-nucleosides: from discovery, synthesis to properties and potential applications. RSC Adv 2019;9:14302–20. https://doi.org/10.1039/C9RA01399G
- 91. Urata H, Shinohara K, Ogura E *et al*. Mirror-image DNA. *J Am Chem Soc* 1991;113:8174–5. https://doi.org/10.1021/ja00021a057
- Venkatesham A, Kachare D, Schepers G et al. Hybridisation potential of 1',3'-di-methylaltropyranoside nucleic acids.
   *Molecules* 2015;20:4020–41.
   https://doi.org/10.3390/molecules20034020
- 93. Wu TF, Nauwelaerts K, Van Aerschot A *et al.* Base-base interactions in the minor groove of double-stranded DNA. *J Org Chem* 2006;71:5423–31. https://doi.org/10.1021/jo052194c
- 94. Martínez-Montero S, Deleavey GF, Martín-Pintado N et al. Locked 2'-deoxy-2',4'-difluororibo modified nucleic acids: thermal stability, structural studies, and siRNA activity. ACS Chem Biol 2015;10:2016–23. https://doi.org/10.1021/acschembio.5b00218
- 95. Malek-Adamian E, Guenther DC, Matsuda S *et al*. 4'-C-methoxy-2'-deoxy-2'-fluoro modified ribonucleotides improve metabolic stability and elicit efficient RNAi-mediated gene silencing. *J Am Chem Soc* 2017;139:14542–55. https://doi.org/10.1021/jacs.7b07582

- 96. Malek-Adamian E, Fakhoury J, Arnold AE *et al.* Effect of sugar 2',4'-modifications on gene silencing activity of siRNA duplexes. *Nucleic Acid Ther* 2019;**29**:187–94. https://doi.org/10.1089/nat.2019.0792
- 97. Bardiot D, Rosemeyer H, Lescrinier E *et al.* Synthesis and properties of oligonucleotides containing 2,4-dihydroxycyclohexyl nucleosides. *Helv Chim Acta* 2005;88:3210–24. https://doi.org/10.1002/hlca.200590258
- 98. Beck KM, Sharma PK, Hornum M *et al.* Double-headed nucleic acids condense the molecular information of DNA to half the number of nucleotides. *Chem Commun* 2021;57:9128–31. https://doi.org/10.1039/D1CC03539H
- Srivastava P, El Asrar RA, Knies C et al. Achiral, acyclic nucleic acids: synthesis and biophysical studies of a possible prebiotic polymer. Org Biomol Chem 2015;13:9249–60.
- 100. Buff R, Hunziker J. 2'-deoxy-2'(S)-ethinyl oligonucleotides: a modification which selectively stabilizes oligoadenylate pairing to DNA complements. *Bioorg Med Chem Lett* 1998;8:521–4. https://doi.org/10.1016/S0960-894X(98)00060-2
- 101. Morita K, Hasegawa C, Kaneko M et al. 2'-,4'-ethylene-bridged nucleic acids (ENA): highly nuclease-resistant and thermodynamically stable oligonucleotides for antisense drug. Bioorg Med Chem Lett 2002;12:73–6. https://doi.org/10.1016/S0960-894X(01)00683-7
- 102. Yamada K, Hariharan VN, Caiazzi J et al. Enhancing siRNA efficacy in vivo with extended nucleic acid backbones. Nat Biotechnol 2025;43:904–13. https://www.nature.com/articles/s41587-024-02336-7
- 103. Damha MJ, Wilds CJ, Noronha A *et al.* Hybrids of RNA and arabinonucleic acids (ANA and 2'F-ANA) are substrates of ribonuclease h. *J Am Chem Soc* 1998;120:12976–7. https://pubs.acs.org/doi/10.1021/ja982325%2B
- 104 . Joyce GF, Schwartz AW, Miller SL *et al*. The case for an ancestral genetic system involving simple analogs of the nucleotides. *Proc Natl Acad Sci USA* 1987;84:4398–402. https://doi.org/10.1073/pnas.84.13.4398
- 105. Dugovic B, Leumann CJ. A 6'-fluoro-substituent in bicyclo-DNA increases affinity to complementary RNA presumably by CF-HC pseudohydrogen bonds. *J Org Chem* 2014;79:1271–9. https://doi.org/10.1021/jo402690j
- 106. Pallan PS, Yu J, Allerson CR et al. Insights from crystal structures into the opposite effects on RNA affinity caused by the S- and R-6'-methyl backbone modifications of 3'-fluoro hexitol nucleic acid. Biochemistry 2012;51:7–9. https://doi.org/10.1021/bi201810r
- 107. Nomura K, An SJ, Kobayashi Y *et al.* Synthesis of 2'-formamidonucleoside phosphoramidites for suppressing the seed-based off-target effects of siRNAs. *Nucleic Acids Res* 2024;52:10754–74. https://doi.org/10.1093/nar/gkae741
- 108. Codington J, Doerr I, Van Praag D et al. Nucleosides. XIV. Synthesis of 2'-deoxy-2'-fluorouridine. J Am Chem Soc 1961;83:5030–1. https://doi.org/10.1021/ja01485a036
- 109. Nguyen HV, Zhao ZY, Sallustrau A et al. A ferrocene nucleic acid oligomer as an organometallic structural mimic of DNA. Chem Commun 2012;48:12165–7. https://doi.org/10.1039/c2cc36428j
- 110. Zhang LL, Peritz A, Meggers E. A simple glycol nucleic acid. J Am Chem Soc 2005;127:4174–5. https://doi.org/10.1021/ja042564z
- 111. Bose T, Kumar VA. Simple molecular engineering of glycol nucleic acid: progression from self-pairing to cross-pairing with cDNA and RNA. *Bioorg Med Chem* 2014;22:6227–32. https://doi.org/10.1016/j.bmc.2014.08.022
- 112. Kitamura Y, Moribe S, Kitade Y. Synthesis of cationic glucosamino nucleic acids for stabilizing oligonucleotides. *Bioorg Med Chem Lett* 2018;28:3174–6. https://doi.org/10.1016/j.bmcl.2018.08.024
- 113. Dempcy RO, Almarsson O, Bruice TC. Design and synthesis of deoxynucleic guanidine - a polycation analog of DNA. Proc Natl

- *Acad Sci USA* 1994;91:7864–8. https://doi.org/10.1073/pnas.91.17.7864
- 114. D'Alonzo D, Van Aerschot A, Guaragna A *et al.* Synthesis and base pairing properties of 1′,5′-anhydro-L-hexitol nucleic acids (L-HNA). *Chem Eur J* 2009;15:10121–31. https://doi.org/10.1002/chem.200901847
- 115. Kerremans L, Schepers G, Rozenski J *et al.* Hybridization between "six-membered" nucleic acids: RNA as a universal information system. *Org Lett* 2001;3:4129–32. https://doi.org/10.1021/ol016183r
- 116. D'Alonzo D, Froeyen M, Schepers G et al. 1',5'-Anhydro-L-ribo-hexitol adenine nucleic acids (α-L-HNA-A): synthesis and chiral selection properties in the mirror image world. J Org Chem 2015;80:5014–22. https://doi.org/10.1021/acs.joc.5b00406
- 117. Hendrix C, Rosemeyer H, Verheggen I *et al.* 1',5'-anhydrohexitol oligonucleotides: synthesis, base pairing, and recognition by regular oligodeoxyribonucleotides and oligoribonucleotides. *Chemistry A European J* 1997;3:110–20. https://doi.org/10.1002/chem.19970030118
- 118. Ceulemans G, VanAerschot A, Rozenski J *et al.* Oligonucleotides with 3-hydroxy-N-acetylprolinol as sugar substitute. *Tetrahedron* 1997;53:14957–74. https://doi.org/10.1016/S0040-4020(97)01047-8
- 119. Augustyns K, Vanaerschot A, Herdewijn P. Synthesis of 1-(2,4-Dideoxy-Beta-D-Erythro-Hexopyranosyl)thymine and its incorporation into oligonucleotides. *Bioorg Med Chem Lett* 1992;2:945–8. https://doi.org/10.1016/S0960-894X(00)80594-6
- 120. D'Alonzo D, Guaragna A, Van Aerschot A *et al.* Toward L-Homo-DNA: stereoselective de novo synthesis of β-L-hexopyranosyl nucleosides. *J Org Chem* 2010;75:6402–10. https://doi.org/10.1021/jo100691y
- 121. Froeyen M, Lescrinier E, Kerremans L *et al.* a-homo-DNA and RNA form a parallel oriented non-A, non-B-type double helical structure. *Chem Eur J* 2001;7:5183–94. https://chemistry-europe.onlinelibrary.wiley.com/doi/10.1002/1521-3765(20011203)7:23%3C5183:: AID-CHEM5183%3E3.0.CO;2-H
- 122. Hossain N, Hendrix C, Lescrinier E et al. Homo-N-nucleosides: incorporation into oligonucleotides and antiviral activity. Bioorg Med Chem Lett 1996;6:1465–8. https://doi.org/10.1016/S0960-894X(96)00254-5
- 123. Sípová H, Springer T, Rejman D et al. 5'-Methylphosphonate nucleic acids-new modified DNAs that increase the RNase H cleavage rate of hybrid duplexes. Nucleic Acids Res 2014;42:5378–89. https://doi.org/10.1093/nar/gku125
- 124. Doboszewski B, Dewinter H, Vanaerschot A *et al.* Synthesis of 3'-deoxy-3'-C-hydroxymethyl-aldopentopyranosyl nucleosides and their incorporation in oligonucleotides. *Tetrahedron* 1995;51,12319–36. https://doi.org/10.1016/0040-4020(95)00777-6
- 125. Christensen UB, Pedersen EB. Intercalating nucleic acids containing insertions of 1-(1-pyrenylmethyl)glycerol: stabilisation of dsDNA and discrimination of DNA over RNA. *Nucleic Acids Res* 2002;30:4918–25. https://doi.org/10.1093/nar/gkf624
- 126 . Gerber AB, Leumann CJ. Synthesis and properties of isobicyclo-DNA. *Chem A Eur J* 2013;19:6990–7006. https://doi.org/10.1002/chem.201300487
- 127. Karri P, Punna V, Kim K et al. Base-pairing properties of a structural isomer of glycerol nucleic acid. Angew Chem Int Ed 2013;52:5840–4. https://doi.org/10.1002/anie.201300795
- 128. Sorensen MD, Kvaerno L, Bryld T *et al.* α-L-configured locked nucleic acid (α-L-LNA): synthesis and properties. *J Am Chem Soc* 2002;**124**:2164–76. https://doi.org/10.1021/ja0168763
- 129. Seth PP, Allerson CR, Berdeja A *et al.* An exocyclic methylene group acts As a bioisostere of the 2'-oxygen atom in LNA. *J Am Chem Soc* 2010;132:14942–50. https://doi.org/10.1021/ja105875e

- 130. Seth PP, Siwkowski A, Allerson CR *et al.* Short antisense oligonucleotides with novel 2'-4' conformationaly restricted nucleoside analogues show improved potency without increased toxicity in animals. *J Med Chem* 2009;52:10–3. https://doi.org/10.1021/jm801294h
- 131. Seth PP, Vasquez G, Allerson CA *et al.* Synthesis and biophysical evaluation of 2',4'-constrained 2'O-methoxyethyl and 2',4'-constrained 2'O-ethyl nucleic acid analogues. *J Org Chem* 2010;75:1569–81. https://doi.org/10.1021/jo902560f
- 132. Summerton J, Weller D. Morpholino antisense oligomers: design, preparation, and properties. Antisense Nucleic A 1997;7:187–95.
- 133. Hossain N, Wroblowski B, Van Aerschot A *et al*. Oligonucleotides composed of 2'-deoxy-1',5'-anhydro-D-mannitol nucleosides with a purine base moiety. *J Org Chem* 1998;63:1574–82. https://doi.org/10.1021/jo9718511
- 134. Van Aerschot A, Meldgaard M, Schepers G et al. Improved hybridisation potential of oligonucleotides comprising o-methylated anhydrohexitol nucleoside congeners. Nucleic Acids Res 2001;29:4187–94. https://doi.org/10.1093/nar/29.20.4187
- 135. Hashimoto H, Switzer C. Self-association of 2',5'-linked deoxynucleotides - meta-DNA. J Am Chem Soc 1992;114:6255–6. https://doi.org/10.1021/ja00041a059
- 136. Kierzek R, He LY, Turner DH. Association of 2'-5' Oligoribonucleotides. *Nucl Acids Res* 1992;20:1685–90. https://doi.org/10.1093/nar/20.7.1685
- 137. Terrazas M, Ocampo SM, Perales JC et al. Effect of bicyclo[3.1.0]hexane 2'-deoxy-pseudosugars on RNA interference: a novel class of siRNA modification. ChemBioChem 2011;12:1056–65. https://doi.org/10.1002/cbic.201000791
- 138. Sabatino D, Damha MJ. Oxepane nucleic acids: synthesis, characterization, and properties of oligonucleotides bearing a seven-membered carbohydrate ring. *J Am Chem Soc* 2007;129:8259–70. https://doi.org/10.1021/ja071336c
- 139. Dueholm KL, Egholm M, Behrens C *et al.* Synthesis of peptide nucleic-acid monomers containing the 4 natural nucleobases thymine, cytosine, adenine, and guanine and their oligomerization. *J Org Chem* 1994;59:5767–73. https://doi.org/10.1021/jo00098a042
- 140. Madhuri V, Kumar VA. Design, synthesis and DNA/RNA binding studies of nucleic acids comprising stereoregular and acyclic polycarbamate backbone: polycarbamate nucleic acids (PCNA). Org Biomol Chem 2010;8,3734–41.
- 141 . Ceulemans G, VanAerschot A, Wroblowski B *et al*.
  Oligonucleotide analogues with 4-hydroxy-N-acetylprolinol as sugar substitute. *Chem A Eur J* 1997;3:1997–2010. https://doi.org/10.1002/chem.19970031215
- 142. Ashley G. Modeling, synthesis, and hybridization properties of-ribonucleic acid. *J Am Chem Soc* 1992;114:9731–6. https://doi.org/10.1021/ja00051a001
- 143 .Efthymiou T, Gavette J, Stoop M *et al.* Chimeric XNA: an unconventional design for orthogonal informational systems. *Chem A Eur J* 2018;24:12811–9. https://doi.org/10.1002/chem.201802287
- 144. Kashida H, Murayama K, Toda T *et al*. Control of the chirality and helicity of oligomers of serinol nucleic acid (SNA) by sequence design. *Angew Chem Int Ed* 2011;50:1285–8. https://doi.org/10.1002/anie.201006498
- 145. Altmann K, Imwinkelried R, Kesselring R *et al.* 1',6'-methano carbocyclic thymidine: synthesis, X-ray crystal structure, and effect on nucleic acid duplex stability. *Tetrahedron Lett* 1994;35:7625–8. https://doi.org/10.1016/S0040-4039(00)78359-6
- 146. Murayama K, Kashida H, Asanuma H. L-threoninol nucleic acid (L-TNA) with suitable structural rigidity cross-pairs with DNA and RNA. *Chem Commun* 2015;51:6500–3. https://doi.org/10.1039/C4CC09244A

- 147. Steffens R, Leumann CJ. Synthesis and thermodynamic and biophysical properties of tricyclo-DNA. *J Am Chem Soc* 1999;121:3249–55. https://doi.org/10.1021/ja983570w
- 148. Inoue N, Minakawa N, Matsuda A. Synthesis and properties of 4'-thioDNA:: unexpected RNA-like behavior of 4'-thioDNA. *Nucleic Acids Res* 2006;34:3476–83. https://doi.org/10.1093/nar/gkl491
- 149. Leydier C, Bellon L, Barascut J et al. 4'-Thio-b-D-oligoribonucleotides: nuclease resistance and hydrogen bonding properties. Nucleos Nucleot Nucleic Acids 1995;14:1027–30.
- 150. Nielsen P, Dreioe LH, Wengel J. Synthesis and evaluation of oligodeoxynucleotides containing acyclic nucleosides introduction of 3 novel analogs and a summary. *Bioorg Med Chem* 1995;3:19–28. https://doi.org/10.1016/0968-0896(94)00143-Q
- 151. Yamada K, Hildebrand S, Davis SM et al. Structurally constrained phosphonate internucleotide linkage impacts oligonucleotide-enzyme interaction, and modulates siRNA activity and allele specificity. Nucleic Acids Res 2021;49:12069–88. https://doi.org/10.1093/nar/gkab1126
- 152. Sasaki S, Yamauchi H, Nagatsugi F et al. W-shape nucleic acid (WNA) for selective formation of non-natural anti-parallel triplex including a TA interrupting site. Tetrahedron Lett 2001;42:6915–8. https://doi.org/10.1016/S0040-4039(01)01446-0
- 153. Rosemeyer H, Seela F.
  1-(2'-Deoxy-Beta-D-Xylofuranosyl)Thyminebuilding-blocks for solid-phase synthesis and properties of Oligo(2'-Deoxyxylonucleotides). *Helv Chim Acta* 1991;74:748–60. https://doi.org/10.1002/hlca.19910740408
- 154. Morvan F, Rayner B, Imbach JL *et al.*, alpha-DNA-V. Parallel annealing, handedness and conformation of the duplex of the unnatural alpha-hexadeoxyribonucleotide alpha-[d(CpApTpGpCpG)] with its beta-complement beta-[d(GpTpApCpGpC)] deduced from high field 1H-NMR. *Nucleic Acids Res* 1987;15:7027–44. https://doi.org/10.1093/nar/15.17.7027
- 155. van de Sande JH, Ramsing NB, Germann MW *et al.* Parallel stranded DNA. *Science* 1988;241:551–7. https://doi.org/10.1126/science.3399890
- 156. Bhan P, Bhan A, Hong M et al. 2',5'-linked oligo-3'-deoxyribonucleoside phosphorothioate chimeras: thermal stability and antisense inhibition of gene expression. Nucleic Acids Res 1997;25:3310–7. https://doi.org/10.1093/nar/25.16.3310
- 157. Wasner M, Arion D, Borkow G *et al.* Physicochemical and biochemical properties of 2',5'-linked RNA and 2',5'-RNA:3',5'-RNA "hybrid" duplexes. *Biochemistry* 1998;37:7478–86. https://doi.org/10.1021/bi980160b
- 158 . Sachse H. Über die konfigurationen der polymethylenringe. *Z Phys Chem* 1892;9U:203–41. https://doi.org/10.1515/zpch-1892-1013
- 159. Kilpatrick J, Pitzer K, Spitzer R. The thermodynamics and molecular structure of cyclopentane. J Am Chem Soc 1947;69:2483–8. https://doi.org/10.1021/ja01202a069
- 160. Altona C, Sundaralingam M. Conformational analysis of the sugar ring in nucleosides and nucleotides. New description using the concept of pseudorotation. *J Am Chem Soc* 1972;94:8205–12. https://doi.org/10.1021/ja00778a043
- 161. Koole L, Buck H, Bazin H et al. Conformational studies of 3'-methyl and 2'-methyl analogues of cordycepin. Tetrahedron 1987;43:2989–97. https://doi.org/10.1016/S0040-4020(01)86838-1
- 162. Li F, Sarkhel S, Wilds CJ *et al.* 2'-Fluoroarabino- and arabinonucleic acid show different conformations, resulting in deviating RNA affinities and processing of their heteroduplexes with RNA by RNase H. *Biochemistry* 2006;45:4141–52. https://doi.org/10.1021/bi052322r

- 163. Cremer D, Pople J. General definition of ring puckering coordinates. *J Am Chem Soc* 1975;97:1354–8. https://doi.org/10.1021/ja00839a011
- 164. Egli M, Pallan PS, Pattanayek R *et al*. Crystal structure of homo-DNA and nature's choice of pentose over hexose in the genetic system. *J Am Chem Soc* 2006;128:10847–56. https://doi.org/10.1021/ja062548x
- 165. Eschenmoser A, Dobler M. Why pentose and not hexose nucleic acids? Part I. Introduction to the problem, conformational analysis of oligonucleotide single strands containing 2',3'-dideoxyglucopyranosyl building blocks ('Homo-DNA'), and reflections on the conformation of A- and B-DNA. Helv Chim Acta 1992;75:218–59.
- 166. Altmann K-H, Kesselring R, Francotte E *et al.* 4',6'-Methano carbocyclic thymidine: a conformationally constrained building block for oligonucleotides. *Tetrahedron Lett* 1994;35:2331–4. https://doi.org/10.1016/0040-4039(94)85212-X
- 167. Wang J, Froeyen M, Hendrix C *et al.* The cyclohexene ring system as a furanose mimic: synthesis and antiviral activity of both enantiomers of cyclohexenylguanine. *J Med Chem* 2000;43:736–45. https://doi.org/10.1021/jm991171l
- 168. Robeyns K, Herdewijn P, Van Meervelt L. Direct observation of two cyclohexenyl (CeNA) ring conformations in duplex DNA. Artif DNA PNA XNA 2010;1:2–8. https://doi.org/10.4161/adna.1.1.10952
- 169. Bocian D, Strauss H. Conformational structure and energy of cycloheptane and some related oxepanes. *J Am Chem Soc* 1977;99:2866–76. https://doi.org/10.1021/ja00451a004
- 170. Espinosa A, Gallo M, Entrena A *et al.* Theoretical conformational analysis of seven-membered rings. V. MM2 and MM3 study of oxepane. *J Mol Struct* 1994;326:249–60. https://doi.org/10.1016/0022-2860(94)08331-2
- 171. Luger P, Buschmann J, Altenrhein C. Structure of oxacyclopentane (oxepane) at 105 K. *Acta Crystallogr C Cryst Struct Commun* 1991;47:102–6. https://doi.org/10.1107/S0108270190000488
- 172. Schlegel MK, Janas MM, Jiang Y *et al.* From bench to bedside: improving the clinical safety of GalNAc-siRNA conjugates using seed-pairing destabilization. *Nucleic Acids Res* 2022;50:6656–70. https://doi.org/10.1093/nar/gkac539
- 173 .Kraka E, Cremer D. Dieter Cremer's contribution to the field of theoretical chemistry. *Int J of Quantum Chem* 2019;**119**:e25849. https://doi.org/10.1002/qua.25849
- 174. Juaristi E. Conformational Behavior of Six-membered Ringsanalysis, Dynamics, and Stereoelectronic Effects. New York: VCH, 1995
- 175. Lescrinier E, Froeyen M, Herdewijn P. Difference in conformational diversity between nucleic acids with a six-membered 'sugar' unit and natural 'furanose' nucleic acids. *Nucleic Acids Res* 2003;31:2975–89. https://doi.org/10.1093/nar/gkg407
- 176. Nauwelaerts K, Lescrinier E, Sclep G *et al.* Cyclohexenyl nucleic acids: conformationally flexible oligonucleotides. *Nucleic Acids Res* 2005;33:2452–63. https://doi.org/10.1093/nar/gki538
- 177. Diekmann S. Definitions and nomenclature of nucleic acid structure parameters. *J Mol Biol* 1989;205:787–91. https://doi.org/10.1016/0022-2836(89)90324-0
- 178. Pallan PS, Lubini P, Egli M. A left-handed supramolecular assembly around a right-handed screw axis in the crystal structure of homo-DNA. *Chem Commun* 2007;43:1447–9. https://doi.org/10.1039/b614983a
- 179. Lu XJ, Olson WK . 3DNA: a software package for the analysis, rebuilding and visualization of three-dimensional nucleic acid structures. *Nucleic Acids Res* 2003;31:5108–21. https://doi.org/10.1093/nar/gkg680
- 180. Robeyns K, Herdewijn P, Van Meervelt L. Structure of the fully modified left-handed cyclohexene nucleic acid sequence GTGTACAC. J Am Chem Soc 2008;130:1979–84. https://doi.org/10.1021/ja077313f

- 181. Schlönvogt I, Pitsch S, Lesueur C *et al.* Pyranosyl-RNA ('p-RNA'): NMR and molecular-dynamics study of the duplex formed by self-pairing of ribopyranosyl-(C-G-A-A-T-T-C-G). *Helv Chim Acta* 1996;79:2316–45. https://doi.org/10.1002/hlca.19960790820
- 182. Declercq R, Van Aerschot A, Read RJ et al. Crystal structure of double helical hexitol nucleic acids. J Am Chem Soc 2002;124:928–33. https://doi.org/10.1021/ja016570w
- 183. Maier T, Przylas I, Strater N *et al.* Reinforced HNA backbone hydration in the crystal structure of a decameric HNA/RNA hybrid. *J Am Chem Soc* 2005;127:2937–43. https://doi.org/10.1021/ja045843v
- 184. Ovaere M, Herdewijn P, Van Meervelt L. The crystal structure of the CeNA:RNA hybrid ce(GCGTAGCG):r(CGCUACGC). Chem A Eur J 2011;17:7823–30. https://doi.org/10.1002/chem.201003594
- 185. Ovaere M, Sponer J, Sponer JE *et al.* How does hydroxyl introduction influence the double helical structure: the stabilization of an altritol nucleic acid:ribonucleic acid duplex. *Nucleic Acids Res* 2012;40:7573–83. https://doi.org/10.1093/nar/gks470
- 186. Johnson AT, Schlegel MK, Meggers E *et al.* On the structure and dynamics of duplex GNA. *J Org Chem* 2011;76:7964–74. https://doi.org/10.1021/jo201469b
- 187. Schlegel MK, Essen LO, Meggers E. Duplex structure of a minimal nucleic acid. *J Am Chem Soc* 2008;130:8158–9. https://doi.org/10.1021/ja802788g
- 188. Rasmussen H, Kastrup JS, Nielsen JN et al. Crystal structure of a peptide nucleic acid (PNA) duplex at 1.7 A resolution. Nat Struct Mol Biol 1997;4:98–101. https://doi.org/10.1038/nsb0297-98
- 189. Kiliszek A, Banaszak K, Dauter Z et al. The first crystal structures of RNA-PNA duplexes and a PNA-PNA duplex containing mismatches-toward anti-sense therapy against TREDs. Nucleic Acids Res 2016;44:1937–43. https://doi.org/10.1093/nar/gkv1513
- 190. Vallazza M, Perbandt M, Klussmann S *et al.* First look at RNA in L-configuration. *Acta Crystallogr D Biol Crystallogr* 2004;60:1–7. https://doi.org/10.1107/S0907444903027690
- 191. Ebert M-O, Luther A, Huynh HK *et al.* NMR solution structure of the duplex formed by self-pairing of -L-arabinopyranosyl-(4'2'-CGAATTCG). *Helv Chim Acta* 2002;85:4055–73. https://onlinelibrary.wiley.com/doi/10.1002/1522-2675(200211) 85:11%3C4055::AID-HLCA4055%3E3.0.CO;2-J
- 192. Kamiya Y, Satoh T, Kodama A et al. Intrastrand backbone-nucleobase interactions stabilize unwound right-handed helical structures of heteroduplexes of L-aTNA/RNA and SNA/RNA. Commun Chem 2020;3:156. https://doi.org/10.1038/s42004-020-00400-2
- 193. Beier M, Reck F, Wagner T *et al.* Chemical etiology of nucleic acid structure: comparing pentopyranosyl-(2'→4') oligonucleotides with RNA. *Science* 1999;283:699–703. https://doi.org/10.1126/science.283.5402.699
- 194. Micura R, Kudick R, Pitsch S et al. Opposite orientation of backbone inclination in pyranosyl-RNA and homo-DNA correlates with Opposite directionality of duplex properties. Angew Chem Int Ed 1999;38:680–3. https://onlinelibrary.wiley.com/doi/10.1002/(SICI)1521-3773(19990301)38:5%3C680::AID-ANIE680%3E3.0.CO;2-C
- 195. Herdewijn P, Marliere P. Toward safe genetically modified organisms through the chemical diversification of nucleic acids. *Chem Biodivers* 2009;6:791–808. https://doi.org/10.1002/cbdv.200900083
- 196. Chaput JC, Herdewijn P, Hollenstein M. Orthogonal genetic systems. *ChemBioChem* 2020;21:1408–11. https://doi.org/10.1002/cbic.201900725
- 197 .Nauwelaerts K, Lescriner E, Herdewijn P. Structure of the  $\alpha$ -Homo-DNA:RNA duplex and the function of twist and slide

- to catalogue nucleic acid duplexes. *Chem A Eur J* 2007;13:90–8. https://doi.org/10.1002/chem.200600363
- 198. Garbesi A, Capobianco ML, Colonna FP *et al.* L-DNAs as potential antimessenger oligonucleotides: a reassessment. *Nucl Acids Res* 1993;21:4159–65. https://doi.org/10.1093/nar/21.18.4159
- 199. Kabsch W, Sander C, Trifonov EN. The ten helical twist angles of B-DNA. *Nucleic Acids Res* 1982;10:1097–104. https://doi.org/10.1093/nar/10.3.1097
- 200. Jaziri F, Maiti M, Lescrinier E et al. Transliteration of a short genetic message from deoxyxylose (dXyloNA) to deoxyribose (DNA) in Escherichia coli. J Systems Chem 2016;7:32–40.
- 201. Eremeeva E, Abramov M, Margamuljana L et al. Chemical morphing of DNA containing four noncanonical bases. Angew Chem Int Ed 2016;55:7515–9. https://doi.org/10.1002/anie.201601529
- 202. Pallan PS, Lybrand TP, Rozners E et al. Conformational morphing by a DNA analogue featuring 7-deazapurines and 5-halogenpyrimidines and the origins of adenine-tract geometry. Biochemistry 2023;62:2854–67. https://doi.org/10.1021/acs.biochem.3c00327
- 203. Ramaswamy A, Froeyen M, Herdewijn P et al. Helical structure of xylose-DNA. J Am Chem Soc 2010;132:587–95. https://doi.org/10.1021/ja9065877
- 204. D'Alonzo D, Amato J, Schepers G *et al.* Enantiomeric selection properties of beta-homoDNA: enhanced pairing for heterochiral complexes. *Angew Chem Int Ed* 2013;**52**:6662–5. https://doi.org/10.1002/anie.201301659
- 205. Gutfreund C, Betz K, Abramov M *et al.* Structural insights into a DNA polymerase reading the xeno nucleic acid HNA. *Nucleic Acids Res* 2025;53:gkae1156. https://doi.org/10.1093/nar/gkae1156
- 206. Schlegel MK, Meggers E. Improved phosphoramidite building blocks for the synthesis of the simplified nucleic acid GNA. *J Org Chem* 2009;74:4615–8. https://doi.org/10.1021/jo900365a
- 207. Nielsen PE. Peptide nucleic acid (PNA): a model structure for the primordial genetic material? *Origins Life Evol Biosphere* 1993;23:323–7. https://doi.org/10.1007/BF01582083
- 208. Schmidt JG, Nielsen PE, Orgel LE. Enantiomeric cross-inhibition in the synthesis of oligonucleotides on a nonchiral template. *J Am Chem Soc* 1997;119:1494–5. https://doi.org/10.1021/ja963563c
- 209. Murayama K, Asanuma H. Design and hybridization properties of acyclic xeno nucleic acid oligomers. *ChemBioChem* 2021;22:2507–15. https://doi.org/10.1002/cbic.202100184
- 210 . Froeyen M, Morvan F, Vasseur JJ *et al.* Conformational and chiral selection of oligonucleotides. *Chem Biodivers* 2007;4:803–17. https://doi.org/10.1002/cbdv.200790065
- 211. Froeyen M, Wroblowski B, Esnouf R *et al.* Molecular-dynamics studies of single-stranded hexitol, altritol, mannitol, and ribose nucleic acids (HNA, MNA, ANA, and RNA, resp.) and of the stability of HNA·RNA, ANA·RNA, and MNA·RNA duplexes. *Helv Chim Acta* 2000;83:2153–82. https://onlinelibrary.wiley.com/doi/10.1002/1522-2675(20000906)83: 9%3C2153::AID-HLCA2153%3E3.0.CO;2-I
- 212. Renneberg D, Leumann CJ. Watson-Crick base-pairing properties of tricyclo-DNA. *J Am Chem Soc* 2002;124:5993–6002. https://pubs.acs.org/doi/10.1021/ja025569%2B
- 213. Meggers E, Zhang L. Synthesis and properties of the simplified nucleic acid glycol nucleic acid. *Acc Chem Res* 2010;43:1092–102. https://doi.org/10.1021/ar900292q
- 214. Egli M, Schlegel MK, Manoharan M. Acyclic (S)-glycol nucleic acid (S-GNA) modification of siRNAs improves the safety of RNAi therapeutics while maintaining potency. *RNA* 2023;29:402–14. https://doi.org/10.1261/rna.079526.122
- 215. Schlegel MK, Matsuda S, Brown CR *et al.* Overcoming GNA/RNA base-pairing limitations using isonucleotides improves the pharmacodynamic activity of ESC+ GalNAc-siRNAs. *Nucleic Acids Res* 2021;49:10851–67. https://doi.org/10.1093/nar/gkab916

- 216. Murayama K, Kashida H, Asanuma H. Acyclic L-threoninol nucleic acid (L-aTNA) with suitable structural rigidity cross-pairs with DNA and RNA. *Chem Commun* 2015;51:6500–3. https://doi.org/10.1039/C4CC09244A
- 217. Haasnoot CA, Altona C. A conformational study of nucleic acid phosphate ester bonds using phosphorus-31 nuclear magnetic resonance. *Nucleic Acids Res* 1979;6:1135–49. https://doi.org/10.1093/nar/6.3.1135
- 218. Florián J, Štrajbl M, Warshel A. Conformational flexibility of phosphate, phosphonate, and phosphorothioate methyl esters in aqueous solution. *J Am Chem Soc* 1998;120:7959–66. https://doi.org/10.1021/ja9710823
- 219. Heinemann U, Rudolph LN, Alings C *et al*. Effect of a single 3'-methylene phosphonate linkage on the conformation of an A-DNA octamer double helix. *Nucleic Acids Res* 1991;19:427–33. https://doi.org/10.1093/nar/19.3.427
- 220. Yang W. Nucleases: diversity of structure, function and mechanism. *Quart Rev Biophys* 2011;44:1–93. https://doi.org/10.1017/S0033583510000181
- 221. Rangarajan ES, Shankar V. Sugar non-specific endonucleases. *FEMS Microbiol Rev* 2001;25:583–613. https://doi.org/10.1111/j.1574-6976.2001.tb00593.x
- 222. Cunningham L, Catlin BW, Garilhe M. A deoxyribonuclease of micrococcus pyogenes. J Am Chem Soc 1956;78:4642–5. https://doi.org/10.1021/ja01599a031
- 223. Cordis GA, Goldblatt PJ, Deutscher MP. Purification and characterization of a major endonuclease from rat liver nuclei. *Biochemistry* 1975;14:2596–603. https://doi.org/10.1021/bi00683a006
- 224. Eckstein F. Phosphorothioates, essential components of therapeutic oligonucleotides. *Nucleic Acid Ther* 2014;24:374–87. https://doi.org/10.1089/nat.2014.0506
- 225. Egli M, Minasov G, Tereshko V et al. Probing the influence of stereoelectronic effects on the biophysical properties of oligonucleotides: comprehensive analysis of the RNA affinity, nuclease resistance, and crystal structure of ten 2'-O-ribonucleic acid modifications. Biochemistry 2005;44:9045–57. https://doi.org/10.1021/bi050574m
- 226. Shaw JP, Kent K, Bird J *et al.* Modified deoxyoligonucleotides stable to exonuclease degradation in serum. *Nucleic Acids Res* 1991;19:747–50. https://doi.org/10.1093/nar/19.4.747
- 227. Hunziker J, Roth H-J, Böhringer M et al. Why pentose- and not hexose-nucleic acids? Part III. Oligo(2',3'-dideoxy-β-D-glucopyranosyl)nucleotides ('Homo-DNA'): base-pairing properties. Helv Chim Acta 1993;76:259–352. https://doi.org/10.1002/hlca.19930760119
- 228. Masquida B, Westhof E. On the wobble GoU and related pairs. *RNA* 2000;6:9–15. https://doi.org/10.1017/S1355838200992082
- 229. Mueller U, Schubel H, Sprinzl M *et al.* Crystal structure of acceptor stem of tRNA(Ala) from Escherichia coli shows unique G.U wobble base pair at 1.16 A resolution. *RNA* 1999;5:670–7. https://doi.org/10.1017/S1355838299982304
- 230 . Hendrix C, Rosemeyer H, De Bouvere B *et al.*1',5'-Anhydrohexitol oligonucleotides: hybridisation and strand displacement with oligoribonucleotides, interaction with RNase H and HIV reverse transcriptase. *Chem A Eur J* 1997;3:1513–20. https://doi.org/10.1002/chem.19970030920
- 231. Miyoshi D, Sugimoto N. Molecular crowding effects on structure and stability of DNA. *Biochimie* 2008;90:1040–51. https://doi.org/10.1016/j.biochi.2008.02.009
- 232. Takahashi S, Herdewijn P, Sugimoto N .. Effect of molecular crowding on DNA polymerase reactions along unnatural DNA templates. *Molecules* 2020;25:4120. https://doi.org/10.3390/molecules25184120
- 233. Bande O, Abu El Asrar R, Braddick D et al. Isoguanine and 5-methyl-isocytosine bases, in vitro and in vivo. Chem A Eur J 2015;21:5009–22. https://doi.org/10.1002/chem.201406392

- 234. Franklin RE, Gosling RG. Molecular configuration in sodium thymonucleate. *Nature* 1953;171:740–1. https://doi.org/10.1038/171740a0
- 235. Saenger W, Hunter WN, Kennard O. DNA conformation is determined by economics in the hydration of phosphate groups. *Nature* 1986;324:385–8. https://doi.org/10.1038/324385a0
- 236. Egli M, Tereshko V, Teplova M et al. X-ray crystallographic analysis of the hydration of A- and B-form DNA at atomic resolution. Biopolymers 1998;48:234–52. https://onlinelibrary.wiley.com/doi/10.1002/(SICI)1097-0282(1998)48:4%3C234::AID-BIP4%3E3.0.CO;2-H
- 237. Shui X, McFail-Isom L, Hu GG *et al.* The B-DNA dodecamer at high resolution reveals a spine of water on sodium. *Biochemistry* 1998;37:8341–55. https://doi.org/10.1021/bi973073c
- 238. Jana B, Pal S, Maiti PK *et al*. Entropy of water in the hydration layer of major and minor grooves of DNA. *J Phys Chem B* 2006;110:19611–8. https://doi.org/10.1021/jp061588k
- 239. Sundaralingam M, Pan B. Hydrogen and hydration of DNA and RNA oligonucleotides. *Biophys Chem* 2002;95:273–82. https://doi.org/10.1016/S0301-4622(01)00262-9
- 240. Timsit Y. DNA structure and polymerase fidelity: a new role for A-DNA. *J Biomol Struct Dyn* 2000;17:169–76. https://doi.org/10.1080/07391102.2000.10506617
- 241. Good L, Sandberg R, Larsson O *et al.* Antisense PNA effects in Escherichia coli are limited by the outer-membrane LPS layer. *Microbiology* 2000;146:2665–70. https://doi.org/10.1099/00221287-146-10-2665
- Nielsen PE. PNA Technology. MB 2004;26:233–48. https://doi.org/10.1385/MB:26:3:233
- 243. Gilbert W. Why genes in pieces? *Nature* 1978;271:501. https://doi.org/10.1038/271501a0
- 244. Doolittle RF. The multiplicity of domains in proteins. *Annu Rev Biochem* 1995;64:287–314. https://doi.org/10.1146/annurev.bi.64.070195.001443
- 245. Petsko GA, Kenyon GL, Gerlt JA *et al.* On the origin of enzymatic species. *Trends Biochem Sci* 1993;18:372–6. https://doi.org/10.1016/0968-0004(93)90091-Z
- 246. Keefe AD, Szostak JW. Functional proteins from a random-sequence library. *Nature* 2001;410:715–8. https://doi.org/10.1038/35070613
- 247. Steitz TA, Smerdon SJ, Jager J *et al.* A unified polymerase mechanism for nonhomologous DNA and RNA polymerases. *Science* 1994;266:2022–5. https://doi.org/10.1126/science.7528445
- 248. Doudna JA, Cech TR. The chemical repertoire of natural ribozymes. *Nature* 2002;418:222–8. https://doi.org/10.1038/418222a
- 249. Breaker RR, Joyce GF. A DNA enzyme that cleaves RNA. Chem Biol 1994;1:223–9. https://doi.org/10.1016/1074-5521(94)90014-0
- 250. Cuenoud B, Szostak JW. A DNA metalloenzyme with DNA ligase activity. *Nature* 1995;375:611–4. https://doi.org/10.1038/375611a0
- 251. Kruger K, Grabowski PJ, Zaug AJ *et al.* Self-splicing RNA: autoexcision and autocyclization of the ribosomal RNA intervening sequence by Tetrahymena. *Cell* 1982;31:147–57. https://doi.org/10.1016/0092-8674(82)90414-7
- 252. Wang Y, Nguyen K, Spitale RC et al. A biologically stable DNAzyme that efficiently silences gene expression in cells. Nat Chem 2021;13:319–26. https://doi.org/10.1038/s41557-021-00645-x
- 253. Nguyen K, Malik TN, Chaput JC. Chemical evolution of an autonomous DNAzyme with allele-specific gene silencing activity. *Nat Commun* 2023;14:2413. https://doi.org/10.1038/s41467-023-38100-9
- 254. Chiba K, Yamaguchi T, Obika S. Development of 8-17 XNAzymes that are functional in cells. *Chem Sci* 2023;14:7620–9. https://doi.org/10.1039/D3SC01928D

- 255. Taylor AI, Pinheiro VB, Smola MJ et al. Catalysts from synthetic genetic polymers. Nature 2015;518:427–30. https://doi.org/10.1038/nature13982
- 256. Wang Y, Ngor AK, Nikoomanzar A *et al.* Evolution of a general RNA-cleaving FANA enzyme. *Nat Commun* 2018;9:5067. https://doi.org/10.1038/s41467-018-07611-1
- 257. Wang Y, Wang Y, Song D *et al.* An RNA-cleaving threose nucleic acid enzyme capable of single point mutation discrimination. *Nat Chem* 2022;14:350–9. https://doi.org/10.1038/s41557-021-00847-3
- 258. Orgel LE. Molecular replication. *Nature* 1992;358:203–9. https://doi.org/10.1038/358203a0
- 259. Inoue T, Orgel LE. Oligomerization of (guanosine 5'-phosphor)-2-methylimidazolide on poly(C). An RNA polymerase model. *J Mol Biol* 1982;162:201–17. https://doi.org/10.1016/0022-2836(82)90169-3
- 260. Giurgiu C, Li L, O'Flaherty DK et al. A mechanistic explanation for the regioselectivity of nonenzymatic RNA primer extension. J Am Chem Soc 2017;139:16741–7. https://doi.org/10.1021/jacs.7b08784
- 261. Sosson M, Pfeffer D, Richert C. Enzyme-free ligation of dimers and trimers to RNA primers. *Nucleic Acids Res* 2019;47:3836–45. https://doi.org/10.1093/nar/gkz160
- 262. Humboldt A, Rami F, Topp FM et al. Prolinyl phosphoramidates of nucleotides with increased reactivity. Angew Chem Int Ed 2024;63:e202319958. https://doi.org/10.1002/anie.202319958
- 263. Schmidt JG, Christensen L, Nielsen PE et al. Information transfer from DNA to peptide nucleic acids by template-directed syntheses. Nucleic Acids Res 1997;25:4792–6. https://doi.org/10.1093/nar/25.23.4792
- 264. Bolli M, Micura R, Eschenmoser A. Pyranosyl-RNA: chiroselective self-assembly of base sequences by ligative oligomerization of tetranucleotide-2',3'-cyclophosphates (with a commentary concerning the origin of biomolecular homochirality). *Chem Biol* 1997;4:309–20. https://doi.org/10.1016/S1074-5521(97)90074-0
- 265. Blain JC, Ricardo A, Szostak JW. Synthesis and nonenzymatic template-directed polymerization of 2'-amino-2'-deoxythreose nucleotides. *J Am Chem Soc* 2014;136:2033–9. https://doi.org/10.1021/ja411950n
- 266. McCloskey CM, Liao JY, Bala S et al. Ligase-mediated threose nucleic acid synthesis on DNA templates. ACS Synth Biol 2019;8:282–6. https://doi.org/10.1021/acssynbio.8b00511
- 267. Zhang W, Kim SC, Tam CP *et al.* Structural interpretation of the effects of threo-nucleotides on nonenzymatic template-directed polymerization. *Nucleic Acids Res* 2021;49:646–56. https://doi.org/10.1093/nar/gkaa1215
- 268. Zhang W, Pal A, Ricardo A *et al*. Template-directed nonenzymatic primer extension using 2-methylimidazole-activated morpholino derivatives of guanosine and cytidine. *J Am Chem Soc* 2019;141:12159–66. https://doi.org/10.1021/jacs.9b06453
- 269. Kozlov IA, De Bouvere B, Van Aerschot A et al. Efficient transfer of information from hexitol nucleic acids to RNA during nonenzymatic oligomerization. J Am Chem Soc 1999;121:5856–9. https://doi.org/10.1021/ja990440u
- 270. Kozlov IA, Zielinski M, Allart B *et al.* Nonenzymatic template-directed reactions on altritol oligomers, preorganized analogues of oligonucleotides. *Chem Eur J* 2000;6:151–5. https://chemistry-europe.onlinelibrary.wiley.com/doi/10.1002/(SICI)1521-3765(20000103)6:1%3C151:: AID-CHEM151%3E3.0.CO;2-H
- 271. Chaput JC, Switzer C. Nonenzymtic oligomerization on templates containing phosphodiester-linked acyclic glycerol nucleic acid analogues. *J Mol Evol* 2000;51:464–70. https://doi.org/10.1007/s002390010109
- 272. Heuberger BD, Switzer C. Nonenzymatic synthesis of RNA by TNA templates. *Org Lett* 2006;8:5809–11. https://doi.org/10.1021/ol062368s

- 273 . Orgel LE. Prebiotic chemistry and the origin of the RNA world. Crit Rev Biochem Mol Biol 2004;39:99–123.
- 274. Pitsch S, Krishnamurthy R, Bolli M *et al.* Pyranosyl-RNA ('p-RNA'): base-pairing selectivity and potential to replicate. *Helv Chim Acta* 1995;78:1621–35. https://doi.org/10.1002/hlca.19950780702
- 275. Bolli M, Micura R, Pitsch S *et al.* Pyranosyl-RNA: further observations on replication. *Helv Chim Acta* 1997;80:1901–51. https://doi.org/10.1002/hlca.19970800613
- 276. Murayama K, Okita H, Kuriki T *et al.* Nonenzymatic polymerase-like template-directed synthesis of acyclic L-threoninol nucleic acid. *Nat Commun* 2021;12:804. https://doi.org/10.1038/s41467-021-21128-0
- 277. Kestemont D, Renders M, Leonczak P et al. XNA ligation using T4 DNA ligase in crowding conditions. Chem Commun 2018;54:6408–11. https://doi.org/10.1039/C8CC02414F
- 278. Vanmeert M, Razzokov J, Mirza MU *et al.* Rational design of an XNA ligase through docking of unbound nucleic acids to toroidal proteins. *Nucleic Acids Res* 2019;47:7130–42. https://doi.org/10.1093/nar/gkz551
- 279. Sabat N, Stampfli A, Hanlon S et al. Template-dependent DNA ligation for the synthesis of modified oligonucleotides. Nat Commun 2024;15:8009. https://doi.org/10.1038/s41467-024-52141-8
- 280. Obexer R, Nassir M, Moody ER *et al.* Modern approaches to therapeutic oligonucleotide manufacturing. *Science* 2024;384:eadl4015. https://doi.org/10.1126/science.adl4015
- 281. Moody ER, Obexer R, Nickl F *et al.* An enzyme cascade enables production of therapeutic oligonucleotides in a single operation. *Science* 2023;380:1150–4. https://doi.org/10.1126/science.add5892
- 282. Flamme M, Hanlon S, Marzuoli I *et al.* Evaluation of 3'-phosphate as a transient protecting group for controlled enzymatic synthesis of DNA and XNA oligonucleotides. *Commun Chem* 2022;5:68. https://doi.org/10.1038/s42004-022-00685-5
- 283. Horning DP, Bala S, Chaput JC *et al.* RNA-catalyzed polymerization of deoxyribose, threose, and arabinose nucleic acids. *ACS Synth Biol* 2019;8:955–61. https://doi.org/10.1021/acssynbio.9b00044
- 284. Sczepanski JT, Joyce GF. A cross-chiral RNA polymerase ribozyme. *Nature* 2014;515:440–2. https://doi.org/10.1038/nature13900
- 285. Joyce GF, Visser GM, van Boeckel CA *et al.* Chiral selection in poly(C)-directed synthesis of oligo(G). *Nature* 1984;310:602–4. https://doi.org/10.1038/310602a0
- 286. Dunn MR, Jimenez RM, Chaput JC. Analysis of aptamer discovery and technology. *Nat Rev Chem* 2017;1:0076. https://doi.org/10.1038/s41570-017-0076
- 287. Zhou J, Rossi J. Aptamers as targeted therapeutics: current potential and challenges. *Nat Rev Drug Discov* 2017;16:181–202. https://doi.org/10.1038/nrd.2016.199
- 288. Keefe AD, Pai S, Ellington AD. Aptamers as therapeutics. *Nat Rev Drug Discov* 2010;9:537–50. https://doi.org/10.1038/nrd3141
- 289. Kavita K, Breaker RR. Discovering riboswitches: the past and the future. *Trends Biochem Sci* 2023;48:119–41. https://doi.org/10.1016/j.tibs.2022.08.009
- 290. Wilson DS, Szostak JW. In vitro selection of functional nucleic acids. *Annu Rev Biochem* 1999;68:611–47. https://doi.org/10.1146/annurev.biochem.68.1.611
- 291. Hermann T, Patel DJ. Adaptive recognition by nucleic acid aptamers. *Science* 2000;287:820–5. https://doi.org/10.1126/science.287.5454.820
- 292. Schofield P, Taylor AI, Rihon J et al. Characterization of an HNA aptamer suggests a non-canonical G-quadruplex motif. Nucleic Acids Res 2023;51:7736–48. https://doi.org/10.1093/nar/gkad592

- 293. Lozoya-Colinas A, Yu Y, Chaput JC. Functionally enhanced XNA aptamers discovered by parallelized library screening. *J Am Chem Soc* 2023;145:25789–96. https://doi.org/10.1021/jacs.3c09497
- 294. Ishino S, Ishino Y. DNA polymerases as useful reagents for biotechnology - the history of developmental research in the field. Front Microbiol 2014;5:465. https://doi.org/10.3389/fmicb.2014.00465
- 295. Wang G, Du Y, Ma X *et al.* Thermophilic nucleic acid polymerases and their application in xenobiology. *Int J Mol Sci* 2022;23:14969. https://doi.org/10.3390/ijms232314969
- 296. Yang W, Gao Y. Translesion and repair DNA polymerases: diverse structure and mechanism. *Annu Rev Biochem* 2018;87:239–61. https://doi.org/10.1146/annurev-biochem-062917-012405
- 297. Chaput JC, Ichida JK, Szostak JW. DNA polymerase-mediated DNA synthesis on a TNA template. *J Am Chem Soc* 2003;125:856–7. https://doi.org/10.1021/ja028589k
- 298. Chaput JC, Szostak JW. TNA synthesis by DNA polymerases. *J Am Chem Soc* 2003;125:9274–5. https://doi.org/10.1021/ja035917n
- 299. Ichida JK, Zou K, Horhota A *et al.* An in vitro selection system for TNA. *J Am Chem Soc* 2005;127:2802–3. https://doi.org/10.1021/ja045364w
- 300. Horhota A, Zou K, Ichida JK et al. Kinetic analysis of an efficient DNA-dependent TNA polymerase. J Am Chem Soc 2005;127:7427–34. https://doi.org/10.1021/ja0428255
- 301. Kempeneers V, Renders M, Froeyen M et al. Investigation of the DNA-dependent cyclohexenyl nucleic acid polymerization and the cyclohexenyl nucleic acid-dependent DNA polymerization. Nucleic Acids Res 2005;33:3828–36. https://doi.org/10.1093/nar/gki695
- 302. Peng CG, Damha MJ. Polymerase-directed synthesis of 2'-deoxy-2'-fluoro-beta-D-arabinonucleic acids. *J Am Chem Soc* 2007;129:5310–1. https://doi.org/10.1021/ja069100g
- 303. Peng CG, Damha MJ. Probing DNA polymerase activity with steroisomeric 2'-fluoro-b-D-arabinose (2'F-araNTPs) and 2'-fluoro-b-D-ribose (2'F-rNTPs) nucleoside 5'-triphosphates. *Can J Chem* 2008;86:881–91. https://doi.org/10.1139/v08-089
- 304. Vastmans K, Froeyen M, Kerremans L et al. Reverse transcriptase incorporation of 1,5-anhydrohexitol nucleotides. Nucleic Acids Res 2001;29:3154–63. https://doi.org/10.1093/nar/29.15.3154
- 305. Kempeneers V, Vastmans K, Rozenski J et al. Recognition of threosyl nucleotides by DNA and RNA polymerases. Nucleic Acids Res 2003;31:6221–6. https://doi.org/10.1093/nar/gkg833
- 306. Jackson LN, Chim N, Shi C *et al.* Crystal structures of a natural DNA polymerase that functions as an XNA reverse transcriptase. *Nucleic Acids Res* 2019;47:6973–83. https://doi.org/10.1093/nar/gkz513
- Nikoomanzar A, Chim N, Yik EJ et al. Engineering polymerases for applications in synthetic biology. Quart Rev Biophys 2020;53:e8. https://doi.org/10.1017/S0033583520000050
- 308. Yu H, Zhang S, Chaput JC. Darwinian evolution of an alternative genetic system provides support for TNA as an RNA progenitor. *Nature Chem* 2012;4:183–7. https://doi.org/10.1038/nchem.1241
- Pinheiro VB, Taylor AI, Cozens C et al. Synthetic genetic polymers capable of heredity and evolution. Science 2012;336:341–4. https://doi.org/10.1126/science.1217622
- Pinheiro VB, Holliger P. The XNA world: progress toward replication and evolution of synthetic genetic polymers. *Curr Opin Chem Biol* 2012;16:245–52. https://doi.org/10.1016/j.cbpa.2012.05.198
- 311. Vallejo D, Nikoomanzar A, Paegel BM *et al.*Fluorescence-activated droplet sorting for single-cell directed evolution. *ACS Synth Biol* 2019;8:1430–40. https://doi.org/10.1021/acssynbio.9b00103
- 312. Maola VA, Yik EJ, Hajjar M *et al.* Directed evolution of a highly efficient TNA polymerase achieved by homologous

- recombination. *Nat Catal* 2024;7:1173–85. https://doi.org/10.1038/s41929-024-01233-1
- 313. Gupta S, Sharma SN, Kundu J *et al.* Morpholino oligonucleotide-mediated exon skipping for DMD treatment: past insights, present challenges and future perspectives. *J Biosci* 2023;48:38. https://doi.org/10.1007/s12038-023-00365-z
- 314. Li N, Xiahou Z, Li Z et al. Identification of hub genes and therapeutic siRNAs to develop novel adjunctive therapy for Duchenne muscular dystrophy. BMC Musculoskelet Disord 2024;25:386. https://doi.org/10.1186/s12891-024-07206-6
- 315. Manoharan M, Akinc A, Pandey RK *et al.* Unique gene-silencing and structural properties of 2'-fluoro-modified siRNAs. *Angew Chem Int Ed* 2011;50:2284–8. https://doi.org/10.1002/anie.201006519
- 316. Schlegel MK, Foster DJ, Kel'in AV *et al.* Chirality dependent potency enhancement and structural impact of glycol nucleic acid modification on siRNA. *J Am Chem Soc* 2017;139:8537–46. https://doi.org/10.1021/jacs.7b02694
- 317. Egli M, Manoharan M. Re-engineering RNA molecules into therapeutic agents. *Acc Chem Res* 2019;52:1036–47. https://doi.org/10.1021/acs.accounts.8b00650
- 318. Schirle NT, Sheu-Gruttadauria J, MacRae IJ .. Gene regulation. Structural basis for microRNA targeting. *Science* 2014;346:608–13. https://doi.org/10.1126/science.1258040
- 319. Matsuda S, Bala S, Liao JY *et al.* Shorter is better: the alpha-(l)-threofuranosyl nucleic acid modification improves stability, potency, safety, and Ago2 binding and mitigates off-target effects of small interfering RNAs. *J Am Chem Soc* 2023;145:19691–706. https://doi.org/10.1021/jacs.3c04744
- 320. Kumar P, Degaonkar R, Guenther DC et al. Chimeric siRNAs with chemically modified pentofuranose and hexopyranose nucleotides: altritol-nucleotide (ANA) containing GalNAc-siRNA conjugates: in vitro and in vivo RNAi activity and resistance to 5'-exonuclease. Nucleic Acids Res 2020;48:4028–40. https://doi.org/10.1093/nar/gkaa125
- 321. Guenther DC, Mori S, Matsuda S *et al.* Role of a "magic" methyl: 2'-deoxy-2'-alpha-F-2'-beta-C-methyl pyrimidine nucleotides modulate RNA interference activity through synergy with 5'-phosphate mimics and mitigation of off-target effects. *J Am Chem Soc* 2022;144:14517–34. https://doi.org/10.1021/jacs.2c01679
- 322. Habibian M, Harikrishna S, Fakhoury J *et al*. Effect of 2'-5'/3'-5' phosphodiester linkage heterogeneity on RNA interference. *Nucleic Acids Res* 2020;48:4643–57. https://doi.org/10.1093/nar/gkaa222
- 323. Yang Y-W, Zhang S, McCullum EO *et al.* Experimental evidence that GNA and TNA were not sequential polymers in the prebiotic evolution of RNA. *J Mol Evol* 2007;65:289–95. https://doi.org/10.1007/s00239-007-9017-9
- 324 . Ranasinghe P, Addison ML, Dear JW *et al.* Small interfering RNA: discovery, pharmacology and clinical development-an introductory review. *Br J Pharmacol* 2023;180:2697–720. https://doi.org/10.1111/bph.15972
- 325. Traber GM, Yu AM. RNAi-based therapeutics and novel RNA bioengineering technologies. J Pharmacol Exp Ther 2023;384:133–54. https://doi.org/10.1124/jpet.122.001234
- 326. Zhang J, Chen B, Gan C *et al.* A comprehensive review of small interfering RNAs (siRNAs): mechanism, therapeutic targets, and delivery strategies for cancer therapy. *IJN* 2023;18:7605–35. https://doi.org/10.2147/IJN.S436038
- 327. Liu M, Wang Y, Zhang Y *et al.* Landscape of small nucleic acid therapeutics: moving from the bench to the clinic as next-generation medicines. *Sig Transduct Target Ther* 2025;10:73. https://doi.org/10.1038/s41392-024-02112-8
- 328. Dhara D, Mulard LA, Hollenstein M. Natural, modified and conjugated carbohydrates in nucleic acids. *Chem Soc Rev* 2025;54:2948–83. https://doi.org/10.1039/D4CS00799A

- 329. Xu Y, Zhu TF. Mirror-image T7 transcription of chirally inverted ribosomal and functional RNAs. *Science* 2022;378:405–12. https://doi.org/10.1126/science.abm0646
- 330. Taylor AI, Beuron F, Peak-Chew SY *et al.* Nanostructures from synthetic genetic polymers. *ChemBioChem* 2016;17:1107–10. https://doi.org/10.1002/cbic.201600136
- 331. Wang Q, Chen X, Li X *et al.* 2'-Fluoroarabinonucleic acid nanostructures as stable carriers for cellular delivery in the strongly acidic environment. *ACS Appl Mater Interfaces* 2020;12:53592–7. https://doi.org/10.1021/acsami.0c11684
- 332. Qin B, Wang Q, Wang Y *et al.* Enzymatic synthesis of TNA protects DNA nanostructures. *Angew Chem Int Ed* 2024;63:e202317334. https://doi.org/10.1002/anie.202317334
- 333. Gasse C, Srivastava P, Schepers G *et al.* Controlled E. coli aggregation mediated by DNA and XNA hybridization. *ChemBioChem* 2023;24,e202300191. https://doi.org/10.1002/cbic.202300191
- 334. Dockerill M, Ford DJ, Angerani S *et al.* Development of supramolecular anticoagulants with on-demand reversibility. *Nat Biotechnol* 2025;43:186–93. https://doi.org/10.1038/s41587-024-02209-z